Analytic View on Coupled Single-Electron Lines

Krzysztof Pomorski[1], Panagiotis Giounanlis[1], Elena Blokhina[1], Dirk Leipold[2], and R. Bogdan Staszewski[1,2]
[1]University College Dublin, Dublin 4, Ireland
[2]Equal1.Labs, Inc., Fremont, CA, USA

***Abstract*—Fundamental properties of two electrostatically interacting single-electron lines (SEL) are determined from a minimalistic tight-binding model. The lines are represented by a chain of coupled quantum wells that could be implemented in a mainstream nanoscale CMOS process technology and tuned electrostatically by DC or AC voltage biases. The obtained results show an essential qualitative difference with two capacitively coupled classical electrical lines. The derived equations and their solutions prove that the two coupled SET lines can create an entanglement between electrons. The correlation function characterizing the correlation/anticorrelation in electron position is introduced both in quantum and classical descriptions of capacitively coupled SELs. The quantum measurement conducted on quantum and classical SELs is described. The difference in quantum and classical ground states can be used as the probe determining the 'quantumness' of the SEL system. The results indicate a possibility of constructing electrostatic (non-spin) coupled qubits that could be used as a building block in a CMOS quantum computer.**

***Index Terms*—Tight-binding model, single-electron lines (SEL), entanglement, insulator-metallic transition, electrostatic interaction, two-body problem, programmable quantum matter, quantum transport, single-electron transistor.**

I. Technological Motivation

The CMOS electronic devices continue to scale down with Moore's law and now are starting to reach the fundamental limitation dictated by the fact that the electron charge is quantized [1], [2], [3]. Moreover, it is commonly accepted by the technologists that the use of fractional electron charge has no practical meaning. On the other hand, the use of different representation of information as by fluxons (quantized flux of magnetic field) in Rapid Single Quantum Flux electronics turns out to have its limitations from the point of view of its size, as implemented in very large scale integration circuits [4]. In this work, we limit ourselves to the electrostatic description of an electron-electron interaction. Current cryogenic CMOS technology development opens up perspectives in implementation of CMOS quantum computer [2], [5] or use of cryogenic CMOS as interface to superconducting quantum circuits [3], [1]. Typical values of capacitances that are implementable in fully depleted silicon-on-insulator (FDSOI) CMOS technology [5] are in the range of 1–10 aF, as depicted in Fig. 1, corresponding to 16–160 mV of the Coulomb blockade voltage.

Fundamentally, the electron quantum properties are captured by the Schrödinger equation that can be obtained in the case of a single electron in effective potential or in the case of many-electron system confined by some local potential. However, the Schrödinger equation in a continuous position space is not the most straightforward approach to capture all electron transport properties on discrete lattices present in various types of metamaterials that can be manufactured on large scale. In this work, we use a tight-binding approximation that can be derived from the Schrödinger equation [7].

II. Mathematical Statement of the Problem

At first, we consider a physical system of an electron confined in a potential with two minima (position-dependent qubit with presence of electron at node 1 and 2) or three minima (position dependent qubit with presence of electron at nodes 1, 2 and 3), as depicted in Fig. 1(A), which was also considered by Fujisawa [8] and Petta [9] and which forms a position-dependent qubit (or qudit). We can write the Hamiltonian in the second quantization as

$$\hat{H}=\sum_{i,j}t_{i\rightarrow j}\hat{a}_i^{\dagger}\hat{a}_j+\sum_i E_p(i)\hat{a}_i^{\dagger}\hat{a}_i+\sum_{i,j}\hat{a}_i^{\dagger}\hat{a}_j^{\dagger}\hat{a}_k\hat{a}_l V_{i,j,k,l}, \tag{1}$$

where $\hat{a}_i^{\dagger}$ is a fermionic creator operator at i-th point in the space lattice and $\hat{a}_j$ is fermionic annihilator operator at j-th point of the lattice. The hopping term $t_{i\rightarrow j}$ describes hopping from i-th to j-th lattice point and is a measure of kinetic energy. The potential $V_{i,j,k,l}$ represents a particle-particle interaction and term $E_p(i)$ incorporates potential energy. In this approach we neglect the presence of a spin. It is convenient to write a system Hamiltonian of position based qubit in spectral form as

$$\begin{aligned}\hat{H}(t)&=E_{p1}(t)\left|1,0\right\rangle\left\langle 1,0\right|+E_{p2}(t)\left|0,1\right\rangle\left\langle 0,1\right|+\\&t_{1\rightarrow 2}(t)\left|0,1\right\rangle\left\langle 1,0\right|+t_{2\rightarrow 1}(t)\left|1,0\right\rangle\left\langle 0,1\right|=\\&=\frac{1}{2}(\hat{\sigma}_0+\hat{\sigma}_3)E_{p1}(t)+\frac{1}{2}(\hat{\sigma}_0-\hat{\sigma}_3)E_{p2}(t)+\\&\frac{1}{2}(\hat{\sigma}_1-i\hat{\sigma}_2)t_{2\rightarrow 1}(t)+\frac{1}{2}(i\hat{\sigma}_2-\hat{\sigma}_1)t_{1\rightarrow 2}(t)\end{aligned} \tag{2}$$

where Pauli matrices are $\hat{\sigma}_0,..,\hat{\sigma}_3$ while system quantum state is given as $\left|\psi(t)\right\rangle=\alpha(t)\left|1,0\right\rangle+\beta(t)\left|0,1\right\rangle$ with $|\alpha|^2+|\beta|^2=1$ and is expressed in Wannier function eigenbases $\left|1,0\right\rangle=w_L(x)$ and $\left|0,1\right\rangle=w_R(x)$ which underlines the presence of electron on the left/right side as equivalent to picture from Schrödinger equation [10].) we obtain two energy eigenstates

$$\left|E_{1(2)}\right\rangle=\begin{pmatrix}\frac{(E_{p2}-E_{p1})\pm\sqrt{4t_{1\rightarrow 2}t_{2\rightarrow 1}+|E_{p1}-E_{p2}|^2}}{2t_{1\rightarrow 2}}\\1\end{pmatrix}=$$

$$\frac{(E_{p2}-E_{p1})\pm\sqrt{4t_{1\rightarrow 2}t_{2\rightarrow 1}+|E_{p1}-E_{p2}|^2}}{2t_{1\rightarrow 2}}\left|1,0\right\rangle+\left|0,1\right\rangle.$$

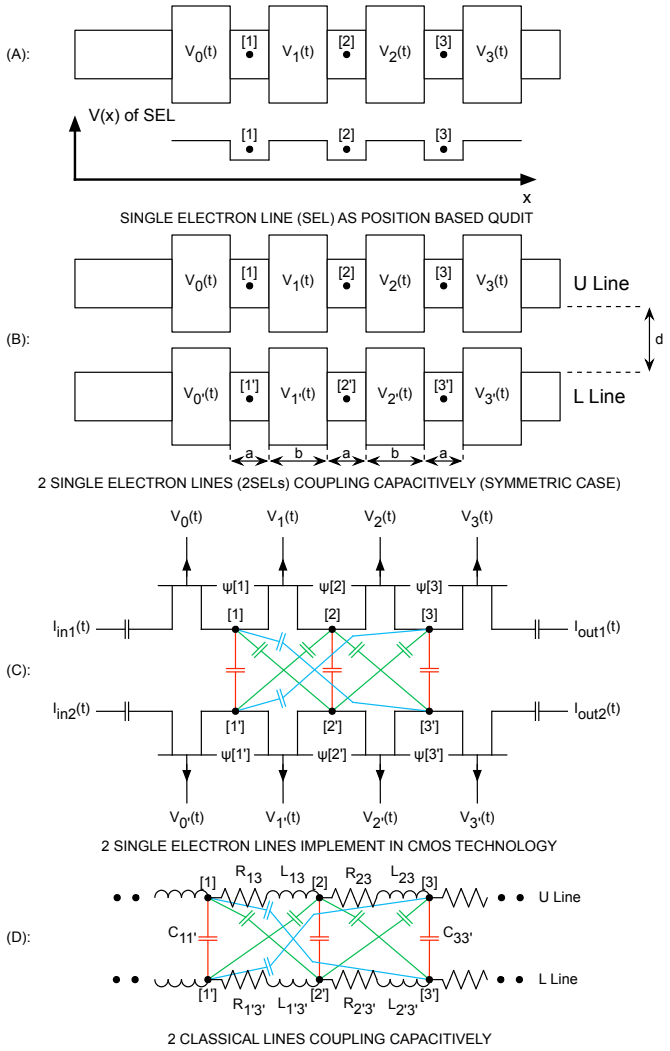

Fig. 1. Nanometer CMOS structure [3], effective potential and circuit representation of: (A) electrostatic position-dependent qubit [10] (the quantum dot dimensions are $80\times80\,\mathrm{nm}^2$ in 22FDX FDSOI CMOS technology); (B)–(C) two electrostatic position-dependent qubits representing two inductively interacting lines (upper "U" and lower "L" quantum systems) in minimalistic way (more rigorously they shall be named as MOS transistor single-electron lines). Presented systems are subjected to the external voltage biasing that controls the local potential landscape in which electrons are confined. Classical limit is expressed by circuit D. 2SEL system is geometrically parameterized by 3 numbers a, b, c.

and energy eigenvalues

$$E_{1(2)} = \frac{1}{2}(E_{p1}+E_{p2} \pm \sqrt{4t_{1\to2}t_{2\to1}+|E_{p1}-E_{p2}|^2}) = \frac{1}{2}(E_{p1}+E_{p2} \pm 2|t_{1\to2}|\sqrt{1+|\frac{E_{p1}-E_{p2}}{2t_{1\to2}t_{2\to1}}|^2}) \approx \frac{1}{2}(E_{p1}+E_{p2} \pm 2|t_{1\to2}|(1+\frac{1}{2}|\frac{E_{p1}-E_{p2}}{2t_{1\to2}t_{2\to1}}|^2)) \approx \frac{1}{2}(E_{p1}+E_{p2}) \pm |t_{1\to2}|. \quad (3)$$

The last approximation is obtained in the limit of $t_{1\to2} \gg E_{p1}, E_{p2}$ (classical limit when system energy becomes big and $|t|$ has the interpretation of kinetic energy) which is the case depicted in the middle Fig.3 when $|t| \to +\infty$. Since Schrödinger formalism can be also applied to the position based qubit that has discrete eigenenergy spectra, one expects that E_p and t_s takes discrete values. It is even more pronounced when one is using formula being the prescription for E_p and t_s parameters as

$$E_p(i) = \int_{-\infty}^{+\infty} \mathrm{d}x \psi_i^*(x) \hat{H}_0 \psi_i(x), \quad (4)$$

where $\psi(x)_i$ is wavefunction of electron localized at i-th node (i-th quantum well) and $\hat{H}$ is effective Hamiltonian. In similar fashion we can define hopping constant from node i-th to node j-th as energy participating in energy transport from one quantum well into the neighbouring quantum well so we define

$$t_{s,i\to j} = \int_{-\infty}^{+\infty} \mathrm{d}x \psi_i^*(x) \hat{H}_0 \psi_j(x), \quad (5)$$

Another interesting fact is the transition from Schrödinger picture to the tight-binding picture can be done by $|\psi\rangle = \int_{-\infty}^{\infty} \psi(x)\mathrm{d}x\,|x\rangle \approx \sum_{k=-\infty}^{k=+\infty} \Delta x \psi(k)\,|k\Delta x\rangle$, where Δx is the distance between nodes. Having a momentum operator defined as $\frac{\hbar}{\Delta x\sqrt{-1}}(-|k+1\rangle\langle k| + |k\rangle\langle k+1|) = \frac{\hbar}{\Delta x\sqrt{-1}}\frac{d}{dx}k$, we obtain the second derivative by Euler formula $(\frac{d^2}{dx^2})_k = \frac{1}{(\Delta x)^2}(|k+1\rangle\langle k| + |k\rangle\langle k+1| - 2\,|k\rangle\langle k|)$. Now we can recover the Schrödinger equation and we observe that $t_{s,i\to i+1} = \frac{\hbar^2}{2m\Delta x}w$, where w is positive and integer. Therefore $t_{s,i\to i+1}$ has positive discrete values. We also observe that the potential in the Schrödinger equation can be connected with $E_p(i) - 2t_{s,i\to i+1} = V_p(i)$ at i-th node. Since kinetic energy is discrete and potential energy in Schrödigner equation is continuous one obtains discrete E_p. The eigenstate depends in the tight binding model on an external vector potential source acting on the qubit by means of $t_{1\to2} = |t_{1\to2}|e^{i\alpha} = t_{2\to1}^*$. Since every energy eigenstate is spanned by $|0,1\rangle$ and $|1,0\rangle$, we will obtain oscillations of occupancy between the two wells [10], [2]. It is worth-mentioning that the act of measurement will affect the qubit quantum state. Since we are dealing with a position-based qubit, we can make measurement of the electron position with the use of an external single-electron device (SED) in close proximity to the qubit. This will require the use of projection operators that represent eigenenergy measurement as $|E_{0(1)}\rangle\langle E_{0(1)}|$ or, for example, measurement of the electron position at left side so we use the projector $|1,0\rangle\langle 0,1|$. We can extend the model for the case of three (and more) coupled wells. In such a case, we obtain the system Hamiltonian for a position based qubit:

$$\hat{H} = \sum_s E_{ps}\,|\mathbf{s}\rangle\langle\mathbf{s}| + \sum_{l,s,s\neq l} t_{s\to l}\,|\mathbf{l}\rangle\langle\mathbf{s}|\,, \quad (6)$$

where $|\mathbf{1}\rangle = |1,0,0\rangle, |\mathbf{2}\rangle = |0,1,0\rangle, |\mathbf{3}\rangle = |0,0,1\rangle$ and its Hamiltonian matrix

$$H(t) = \begin{pmatrix} E_{p1}(t) & t_{2\to1}(t) & t_{3\to1}(t) \\ t_{1\to2}(t) & E_{p2}(t) & t_{3\to2}(t) \\ t_{1\to3}(t) & t_{2\to3}(t) & E_{p3}(t) \end{pmatrix} \quad (7)$$

and quantum state $|\psi\rangle$ (with a normalization condition $|\alpha|^2+|\beta|^2+|\gamma|^2=1$) is given as

$$|\psi\rangle=\begin{pmatrix}\alpha(t)\\ \beta(t)\\ \gamma(t)\end{pmatrix}=\alpha(t)\,|1,0,0\rangle+\beta(t)\,|0,1,0\rangle+\gamma(t)\,|0,0,1\rangle\,.$$

Coefficients $\alpha(t)$, $\beta(t)$ and $\gamma(t)$ describe oscillations of occupancy of one electron at wells 1, 2 and 3. The problem of qubit equations of motion can be formulated by having $|\psi\rangle = c_1(0)e^{-\frac{i}{\hbar}tE_1}|E_1\rangle + c_2(0)e^{-\frac{i}{\hbar}tE_2}|E_2\rangle + c_3(0)e^{-\frac{i}{\hbar}tE_3}|E_3\rangle$, where $|c_1(0)|^2$,$|c_2(0)|^2$ and $|c_3(0)|^2$ are probabilities of occupancy of E_1, E_2 and E_3 energetic levels. Energy levels are the roots of 3rd order polynomial

$$\begin{aligned}(-E_{p1}E_{p2}E_{p3}+E_{p3}t_{12}^2+E_{p1}t_{23}^2+E_{p2}t_{13}^2-2t_{s12}t_{s13}t_{s23})\\ +(E_{p1}E_{p2}+E_{p1}E_{p3}+E_{p2}E_{p3}-t_{12}^2-t_{23}^2-t_{13}^2)E\\ -(E_{p1}+E_{p2}+E_{p3})E^2+E^3=0,\end{aligned}$$

where $|E_1\rangle, |E_2\rangle, |E_3\rangle$ are 3-dimensional Hamiltonian eigenvectors.

By introducing two electrostatically interacting qudits, we are dealing with the Hamiltonian of the upper and lower lines as well as with their Coulomb electrostatic interactions. We are obtaining the Hamiltonian in spectral representation acting on the product of Hilbert spaces in the form of $\hat{H}=\hat{H}_U\times I_L+I_U\times\hat{H}_L+\hat{H}_{U-L}$ where H_u and H_l are Hamiltonians of separated upper and lower qudits, H_{l-u} is a two-line Coulomb interaction and $I_{u(l)}=|1,0,0\rangle_{u(l)}\langle 1,0,0|_{u(l)}+|0,1,0\rangle_{u(l)}\langle 0,1,0|_{u(l)}+|0,0,1\rangle_{u(l)}\langle 0,0,1|_{u(l)}$. The electrostatic interaction is encoded in $E_c(1,1')=E_c(2,2')=E_c(3,3')=\frac{e^2}{4\pi\epsilon_0\epsilon d}=q_1$ (red capacitors of Fig. 1) and $q_2=E_c(2,1')=E_c(2,3')=E_c(1,2')=E_c(3,2')=\frac{e^2}{4\pi\epsilon_0\epsilon\sqrt{d^2+(a+b)^2}}$ and electrostatic energy of green capacitors of Fig. 1 is

$$^{(8)}E_c(1,3')=E_c(3,1')=q_2=\frac{e^2}{4\pi\epsilon_0\epsilon\sqrt{d^2+4(a+b)^2}},\quad(9)$$

where a, b and d are geometric parameters of the system, $q=e$ is electron charge and ϵ is a relative dielectric constant of the material; ϵ_0 corresponds to the dielectric constant of vacuum. The very last Hamiltonian corresponds to the following quantum state $|\psi(t)\rangle$ ($|\gamma_1(t)|^2+..|\gamma_9(t)|^2=1$) given as

$$\begin{aligned}|\psi(t)\rangle=\gamma_1(t)\,|1,0,0\rangle_u|1,0,0\rangle_l+\gamma_2(t)\,|1,0,0\rangle_u|0,1,0\rangle_l\\ +\gamma_3(t)\,|1,0,0\rangle_u|0,0,1\rangle_l+\gamma_4(t)\,|0,1,0\rangle_u|1,0,0\rangle_l\\ +\gamma_5(t)\,|0,1,0\rangle_u|0,1,0\rangle_l+\gamma_6(t)\,|0,1,0\rangle_u|0,0,1\rangle_l\\ +\gamma_7(t)\,|0,0,1\rangle_u|0,0,1\rangle_l+\gamma_8(t)\,|0,0,1\rangle_u|0,1,0\rangle_l\\ +\gamma_9(t)\,|0,0,1\rangle_u|0,0,1\rangle_l\,,\end{aligned}\quad(10)$$

where $|\gamma_1(t)|^2$ is the probability of finding two electrons at nodes 1 and 1' at time t (since γ_1 spans $|1,0,0\rangle_u|1,0,0\rangle_l$), etc. The Hamiltonian has nine eigenenergy solutions that are parametrized by geometric factors and hopping constants $t_{k,m}$ as well as energies $E_p(k)$ for the case of 'u' or 'l' system. Formally, we can treat $E_p(k)=t_{k\to k}\equiv t_{k,k}\equiv t_k\in\mathbf{R}$ as a hopping from k-th lattice point to the same lattice point k. We obtain the following Hamiltonian

$$\hat{H}=\begin{pmatrix}\xi_{1,1'} & t_{1'\to2'} & t_{1'\to3'} & t_{1\to2} & 0 & 0 & t_{1\to3} & 0 & 0\\ t_{2'\to1'} & \xi_{1,2'} & t_{2'\to3'} & 0 & t_{1\to2} & 0 & 0 & t_{1\to3} & 0\\ t_{3'\to1'} & t_{3'\to2'} & \xi_{1,3'} & 0 & 0 & t_{1\to2} & 0 & 0 & t_{1\to3}\\ t_{2\to1} & 0 & 0 & \xi_{2,1'} & t_{1'\to2'} & t_{1'\to3'} & t_{2\to3} & 0 & 0\\ 0 & t_{2\to1} & 0 & t_{2'\to1'} & \xi_{2,2'} & t_{2'\to3'} & 0 & t_{2\to3} & 0\\ 0 & 0 & t_{2\to1} & t_{3'\to1'} & t_{3'\to2'} & \xi_{2,3'} & 0 & 0 & t_{2\to3}\\ t_{3\to1} & 0 & 0 & t_{3\to2} & 0 & 0 & \xi_{3,1'} & t_{1'\to2'} & t_{1'\to3'}\\ 0 & t_{3\to1} & 0 & 0 & t_{3\to2} & 0 & t_{2'\to1'} & \xi_{3,2'} & t_{2'\to3'}\\ 0 & 0 & t_{3\to1} & 0 & 0 & t_{3\to2} & t_{3'\to1'} & t_{3'\to2'} & \xi_{3,3'}\end{pmatrix}=\begin{pmatrix}H(1)_{1',3'} & H_{1,2} & H_{1,3}\\ H(1)_{2,1} & H(2)_{1',3'} & H_{2,3}\\ H_{3,1} & H_{3,2} & H(3)_{1,3'}\end{pmatrix}\quad(11)$$

with diagonal elements $([\xi_{1,1'},\xi_{1,2'},\xi_{1,3'}]\,,[\xi_{2,1'},\xi_{2,2'},\xi_{2,3'}],[\xi_{3,1'},\xi_{3,2'},\xi_{3,3'}])$ set to $([(E_{p1}+E_{p1'}+E_c(1,1')),(E_{p1}+E_{p2'}+E_c(1,2'))\,,(E_{p1}+E_{p3'}+E_c(1,3'))],[((E_{p1}+E_{p1'}+E_c(1,1')),(E_{p2}+E_{p2'}+E_c(2,2'))\,,(E_{p2}+E_{p3'}+E_c(2,3'))],[((E_{p3}+E_{p1'}+E_c(3,1'),(E_{p3}+E_{p2'}+E_c(3,2')),(E_{p3}+E_{p3'}+E_c(3,3'))])$. In the absence of magnetic field, we have $t_{k\to m}=t_{m\to k}=t_{k,m}=t_{m,k}\in\mathbf{R}$ and in the case of nonzero magnetic field $t_{k,m}=t_{m,k}^*\in\mathbf{C}$. It is straightforward to determine the matrix of two lines with N wells [=3 in this work] each following the mathematical structure of two interacting lines with three wells in each line. Matrices $H_{1,2},H_{2,3},H_{1,3}$ are diagonal of size $N\times N$ with all the same terms on the diagonal. At the same time, matrices $H(1)_{1',N'}$,..,$H(N)_{1',N'}$ have only different diagonal terms corresponding to $((\xi_{1,N'},..,\xi_{1,N'}),..,((\xi_{N,N'},..,\xi_{N,N'})$ elements. In simplified considerations we can set $t_{1\to N}=t_{N\to1}$ and $t_{1'\to N'}=t_{N'\to1'}$ to zero since a probability for the wavefunction transfer from 1st to N-th lattice point is generally proportional to $\approx\exp(-sN)$, where s is some constant. It shall be underlined that in the most general case

of two capacitively coupled symmetric SELs with three wells each (being parallel to each other), we have six (all different $E_p(k)$ and $E_p(l')$) plus six (all different $t_{k\to s}$, $t_{k'\to s'}$) plus three geometric parameters (d, a and b) as well as a dielectric constant hidden in the effective charge of interacting electrons e. Therefore, the model Hamiltonian has 12+4 real-valued parameters (four depend on the material and geometry of 2 SELs). They can be extracted from a particular transistor implementation of two SELs (Fig. 1C). There are two main physically important regimes when $t \ll E_p$ and when $t \gg E_p$. They respectively correspond to the case of electron tunneling from one quantum well into another (the electron is not in highly excited state) and the case when the electron's wavepacket can move freely between neighboring wells (electron is in highly excited state).

III. Analytical and Numerical Modeling of Capacitively Coupled SELs

A. Analytical Results

The greatest simplification of matrix (7) is when we set all $t_{k'\to m'} = t_{o\to m} = |t|$, and all $E_p(k) = E_p(m') = E_p$ for N=3. Let us first consider the case of two insulating lines (all wells on each line are completely decoupled so there is no electron tunneling between the barriers and the barrier energies are high) where there are trapped electrons so $|t| = 0$ (electrons are confined in quantum wells and cannot move towards neighbouring wells). In such a case, we deal with a diagonal matrix that has three different eigenvalues on its diagonal and has three different eigenenergy values

$$\hat{E} = \begin{cases} E_1 = q_1 = E_p + \frac{e^2}{4\pi\epsilon\epsilon_0 d}, \\ E_2 = q_2 = E_p + \frac{e^2}{4\pi\epsilon\epsilon_0\sqrt{|d|^2+(a+b)^2}}, \\ E_3 = q_3 = E_p + \frac{e^2}{4\pi\epsilon\epsilon_0\sqrt{|d|^2+4(a+b)^2}}, \end{cases} \tag{12}$$

so $E_3 < E_2 < E_1$. In the limit of infinite distance d between SELs, we have nine degenerate eigenergies. They are set to E_{pk} which corresponds to six decoupled quantum systems (the first electron is delocalized into three upper wells, while the second electron is delocalized into three lowers wells).

Let us also consider the case of ideal metal where electrons are completely delocalized. In such a case, all $t_{k(k')} \gg E_{pl(s)}$ which brings Hamiltonian diagonal terms to be negligible in comparison with other terms. In such a case, we can set all diagonal terms to be zero which is an equivalent to the case of infinitely spaced SELs lines. It simply means that in the case of ideal metals, two lines are not 'seeing' each other.

Let us now turn to the case where processes associated with hopping between wells have similar values of energy to the energies denoted as $E_{pk(l')}$. In such a case, the Hamiltonian matrix can be parametrized only by three real value numbers due to symmetries depicted in Fig. 1B (we divide the matrix by a constant number $|t|$) so

$$\begin{cases} q_{1_1} = \frac{2E_p+\frac{e^2}{d}}{|t|}, \\ q_{1_2} = \frac{2E_p+\frac{e^2}{\sqrt{d^2+(a+b)^2}}}{|t|}, \\ q_{1_3} = \frac{2E_p+\frac{e^2}{\sqrt{d^2+4(a+b)^2}}}{|t|}. \end{cases}$$

For a fixed $|t|$, we change the distance d and observe that q_{1_1} can be arbitrary large, while q_{1_2} and q_{1_3} have finite values for d=0. Going into the limit of infinite distance d, we observe that all q_{1_1}, q_{1_2} and q_{1_3} approach a finite value $\frac{2E_p}{|t|}$. We obtain the simplified Hamiltonian matrix (renormalized Hamiltonian as $\hat{H}_r = \frac{1}{|t|}\hat{H}$) that is a Hermitian conjugate and has a property $H_{k,k} = H_{N-k+1,N-k+1}$. It is in the form

$$\hat{H}_r = \begin{pmatrix} q_{1_1} & 1 & 0 & 1 & 0 & 0 & 0 & 0 & 0 \\ 1 & q_{1_2} & 1 & 0 & 1 & 0 & 0 & 0 & 0 \\ 0 & 1 & q_{1_3} & 0 & 0 & 1 & 0 & 0 & 0 \\ 1 & 0 & 0 & q_{1_2} & 1 & 0 & 1 & 0 & 0 \\ 0 & 1 & 0 & 1 & q_{1_1} & 1 & 0 & 1 & 0 \\ 0 & 0 & 1 & 0 & 1 & q_{1_2} & 0 & 0 & 1 \\ 0 & 0 & 0 & 1 & 0 & 0 & q_{1_3} & 1 & 0 \\ 0 & 0 & 0 & 0 & 1 & 0 & 1 & q_{1_2} & 1 \\ 0 & 0 & 0 & 0 & 0 & 1 & 0 & 1 & q_{1_1} \end{pmatrix} \tag{13}$$

We can analytically find nine energy eigenvalues and they correspond to the entangled states. We have

$$\begin{cases} E_1 = q_{1_1}, \\ E_2 = q_{1_2}, \\ E_3 = \frac{1}{2}(q_{1_1} + q_{1_2} - \sqrt{8 + (q_{1_1} - q_{1_2})^2}), \\ E_4 = \frac{1}{2}(q_{1_1} + q_{1_2} + \sqrt{8 + (q_{1_1} - q_{1_2})^2}), \\ E_5 = \frac{1}{2}(q_{1_2} - q_{1_3} - \sqrt{8 + (q_{1_2} - q_{1_3})^2}), \\ E_6 = \frac{1}{2}(q_{1_2} - q_{1_3} + \sqrt{8 + (q_{1_2} - q_{1_3})^2}). \end{cases} \tag{14}$$

The last 3 energy eigenvalues are the most involving analytically and are the roots of a 3rd order polynomial

$$(2q_{1_1} + 6q_{1_3} - q_{1_1}q_{1_2}q_{1_3}) + (-8 + q_{1_1}q_{1_2} + q_{1_1}q_{1_3} + q_{1_2}q_{1_3})E_k - (q_{1_1} + q_{1_2} + q_{1_3})E_k^2 + E_k^3 = 0. \tag{15}$$

We omit writing direct and very lengthy formulas since the solutions of a 3rd-order polynomial are commonly known. The eigenvectors have the structure given in Appendix VI.

We can readily recognize that all nine energy eigenvectors are entangled. In particular, the first two eigenenergy states (given also in formula (48)) are a linear combination of position-dependent states,

$$\begin{aligned} |E_1\rangle &= |1,0,0\rangle_U |1,0,0\rangle_L - |0,1,0\rangle_U |0,1,0\rangle_L + \\ &\quad |0,0,1\rangle_U |0,0,1\rangle_L , \\ |E_2\rangle &= |1,0,0\rangle_U |0,1,0\rangle_L - |0,1,0\rangle_U |1,0,0\rangle_L \\ &\quad - |0,1,0\rangle_U |0,0,1\rangle_L + |0,0,1\rangle_U |0,1,0\rangle_L , \end{aligned} \tag{16}$$

so they have no equivalence in the classical picture of two charged balls in channels that are repelling each other.

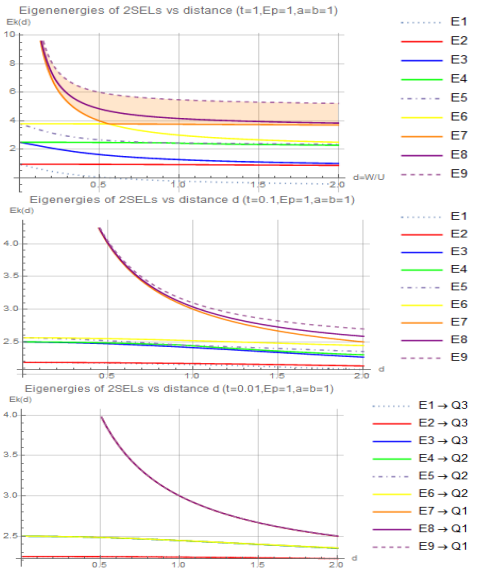

Fig. 2. Cases of: (a) metal ($t = 1, E_p = 1$); (b) semiconductor ($t = 0.1, E_p = 1$); and (c) insulator ($t = 0.01, E_p = 1$) state of 2-SELs given by eigenenergy spectra as function of distance d between two lines ($a = b = 1, e = 1$).

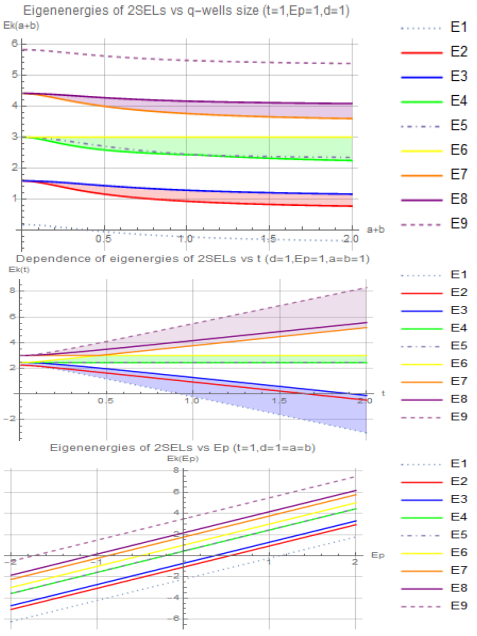

Fig. 3. Dependence of eigenenergy spectra vs. (a) quantum well size $a + b$, (b) hopping term $|t|$, and (c) chemical potential E_p parameter.

B. Numerical Results for Case of Capacitively Coupled SETs

At first, we are analyzing available spectrum of eigenenergies as in the case of insulator-to-metal phase transition [11], which can be implemented in a tight-binding model by a systematic increase of the hopping term from small to large values, while at the same time keeping all other parameters constant, as depicted in Fig. 3. The described tight-binding model can mimic a metal (t=1), semiconductor (t=0.1) or insulator state (t=0.01), as given in Fig. 2. We can recognize 2-SELs' eigen-energy spectra dependence on the distance between the two lines. Characteristic narrowing of bands is observed when one lowers distance d between SELs (which can be related to the ratio of W/U in the Hubbard model) and it is one of the signs of transition from metallic to insulator regime (Mott-insulator phase transition [11]). One of the plots referring to $t = 0.01$ describes Anderson localization of electrons and, in such a case, energy eigenspectra are determined by formula (12) and the hopping terms t can be completely neglected since the electrons are localized in the quantum-well potential minima.

Bottom plots of Fig. 3 describe the ability of tunneling eigenenergy spectra with respect to the quantum well $(a + b)$, E_p and t parameters. The last two parameters can be directly controlled by an applied voltage as earlier shown in Fig. 1, where eight voltage signals are used for controlling the effective tight-binding Hamiltonian. It is informative to notice that a change in the quantum well length, expressed by $a + b$, would not affect the eigenenergy of 2-SELs significantly. The observed change affects the ratio of electrostatic to kinetic energy and thus is similar to the change in energy eigenspectra generated by different distances d. We can spot narrowing of the bands when moving from the situation of lower to higher electrostatic energy of interacting electron and, again, it is typical for the metal-insulator phase transition. Change of the ratio of the kinetic to electrostatic energy can be obtained by keeping constant the quantum well size and the distance between the two SELs, while changing the hopping constant t which is a measure of the electron ability in conducting electric or heat current. Again, we observe the narrowing of bands when we reduce t so the dominant energy of electron is due to the electron-electron interaction. The last plot of Fig. 3 describes our ability of tunneling eigenenergy spectra of the system in a linear way just by changing of the E_p parameter. In a very real, way we can recognize the ability of tuning the chemical potential (equivalent to Fermi energy at temperature T=0K) by controlling the voltages given in Fig.1 in our artificial lattice system. Due to the controllability of energy eigenspectra by the controlling voltages, from Fig. 1 one can recognize 2-SEL system as the first stage of implementation of programmable quantum matter. In the general case of considered 2-SELs, the Hamiltonian consists of 12 different E_p parameters and 6 different t parameters that can be controlled electrostatically (18 parameters under electrostatic control) by 2-SELs controlling voltages $V_0(t), .., V_3(t), V_{0'}(t), .., V_{3'}(t)$ depicted in Fig. 1.

The numerical modeling of electron transport across the coupled SELs is about solving a set of nine coupled recurrent equations of motion as it is in the case of the time-dependent 2-SEL Hamiltonian. In this work, we consider time-independent Hamiltonian, implying constant occupation of energetic levels. Therefore, the quantum state can be written in the form $|\psi(t')\rangle$

$= \alpha_1 e^{\frac{\hbar}{i}E_1 t'} |E_1\rangle + \ldots + \alpha_9 e^{\frac{\hbar}{i}E_9 t'} |E_9\rangle$, so the probability of occupancy of energetic level E_1 is $|\alpha_1|^2 = |\langle E_1 | \psi(t)\rangle|^2 = p_{E1} = constant$, etc. Since we have obtained the analytical form of all states $|E_k\rangle$ and eigenenergies E_k, we have the analytical form of quantum state dynamics $|\psi(t')\rangle$ with time. From the obtained analytical solutions presented in Appendix VI, we recognize that every eigenenergy state is a linear combination of position-based states $|k\rangle \bigotimes |l'\rangle$, which implies that the quantum state can never be fully localized at two nodes k and l' as it is pointed out by the analytically obtained eigenstates of the 2-SEL Hamiltonian given in Appendix VI.

In the conducted numerical simulations we visualize analytical solutions. We set $\hbar = 1$ and $\alpha_1 = \ldots = \alpha_8 = \frac{1}{9}$, $\alpha_9 = \sqrt{1 - \frac{8}{81}}$ (Scenario I that has populated all nine energetic levels) or $\alpha_1 = \alpha_2 = \frac{1}{2}$,$\alpha_9 = \frac{\sqrt{2}}{2}$,$\alpha_3 = \ldots = \alpha_8$ (Scenario II that has populated three energetic levels) that will correspond to the top or bottom plots of Fig. 4. We can recognize that probability of occupancy of (1,1') from Fig. 1 (when two electrons are at input of 2-SEL) is given by $|(\langle 1,0,0| \bigotimes \langle 1,0,0|) |\psi(t)\rangle|^2 = |\gamma_1(t)|^2 = p_1(t)$ (two electrons as the SEL inputs) can be compared with occupancy of (3,3') given by $p_9(t) = |\gamma_9(t)|^2 = |(\langle 0,0,1| \bigotimes \langle 0,0,1|) |\psi(t)\rangle|^2$ (two electrons at the SEL outputs) as depicted in Fig. 4. It is relatively easy to identify probability of finding the first electron at input as the sum of $p_1(t) + p_2(t) + p_3(t)$.

Various symmetries can be traced in Scenario II (nine populated energy levels) given by Fig. 4 as between probability $p_2(t)$ and $p_8(t)$ or in the upper part of Fig. 4 in Scenario I (three populated energy levels) when $p_2(t) = p_8(t)$ or $\phi_2(t) = phase(\gamma_2(t)) = \phi_8(t)$. The same symmetry relations apply to the case of probability $p_4(t)$ and $p_6(t)$ as well as $\phi_4(\gamma_4(t))$ and $\phi_6(\gamma_6(t))$. These symmetries have their origin in the fact that the 2-SEL system is symmetric along the x-axis which can be recognized in the symmetries of simplified Hamiltonian matrix (13). It shall be underlined that in the most general case, when the system matrix has no symmetries, the energy eigenspectra might have less monotonic behavior.

C. Act of Measurement and Dynamics of Quantum State

The quantum system dynamics over time is expressed by the equation of motion $\hat{H}(t') |\psi(t')\rangle = i\hbar \frac{d}{dt'} |\psi(t')\rangle$ that can be represented in a discrete-time step by the relation

$$\frac{dt'}{i\hbar} \hat{H}(t') |\psi(t')\rangle + |\psi(t')\rangle = |\psi(t' + dt')\rangle \,. \qquad (17)$$

It leads to the following equations of motion for the quantum state expressed by equation (10) as follows

$$\vec{\gamma}(t' + dt') = \left\{ \begin{array}{l} \gamma_1(t') + dt' \sum_{k=1}^{9} \hat{H}_{1,k}(t') \gamma_k(t') = \\ f_1(\vec{\gamma}(t'), dt')[\hat{H}(t')], \\ .. \\ \gamma_9(t') + dt' \sum_{k=1}^{9} \hat{H}_{9,k}(t') \gamma_k(t') = \\ f_9(\vec{\gamma}(t'), dt')[\hat{H}(t')] \end{array} \right\} =$$
$$= \vec{f}(\vec{\gamma}(t'), dt')[\hat{H}(t')] = \vec{f}(\vec{\gamma}(t'), dt')_{[\hat{H}(t')]}. \qquad (18)$$

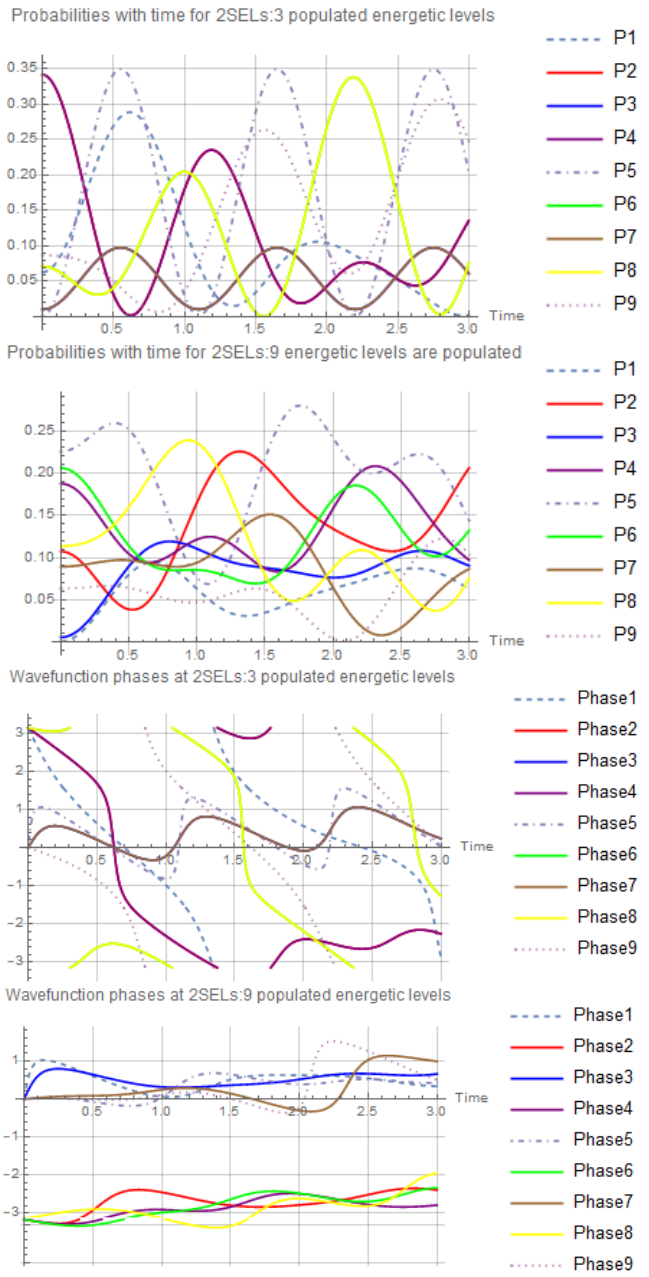

Fig. 4. Quantum state of two SELs over time: Upper (Lower) plots populate 3 (9) energy levels as given by Scenario I (Scenario II). The probabilities of finding both electrons simultaneously at the input $p_1(t) = |\gamma_1(t)|^2$ and output $p_9(t) = |\gamma_1(t)|^2$ is shown with time as well as evolution of phases $\phi_1(t), .., \phi_9(t)$ of $\gamma_1(t) = |\gamma_1(t)|e^{\phi_1(t)}$, .., $\gamma_9(t) = |\gamma_9(t)|e^{\phi_9(t)}$ corresponding to equation (10).

Symbol [.] denotes a functional dependence of $\vec{f}(\vec{\gamma}(t'),dt')$ on Hamiltonian $\hat{H}(t')$. The measurement can be represented by projection operators $\hat{\Pi}(t')$ equivalent to the matrix that acts on the quantum state over time. The lack of measurement can simply mean that the state projects on itself so the projection is the identity operation ($\hat{\Pi}(t')=\hat{I}_{9\times 9}$). Otherwise, the quantum state is projected on its subset and hence the projection operator can change in a non-continuous way over time. We can formally write the quantum state dynamics with respect to time during the occurrence of measurement process (interaction of external physical system with the considered quantum system) as

$$\vec{\gamma}(t'+dt')=\frac{\hat{\Pi}(t'+dt')(\vec{f}(\vec{\gamma}(t'),dt'))}{(\hat{\Pi}(t'+dt')\vec{f}(\vec{\gamma}(t'),dt'))^{\dagger}(\hat{\Pi}(t'+dt')\vec{f}(\vec{\gamma}(t'),dt'))}. \quad (19)$$

Let us refer to some example by assuming that a particle in the upper SELs was detected by the upper output detector (Fig. 1b). In such a case, the following projector $\hat{\Pi}(t,t+\Delta t)$ is different from the identity in time interval $(t,t+\Delta t)$ with $1_{1_{t,t+\Delta t}}=1$ set to 1 in this time interval and 0 otherwise. The projector acts on the quantum state (diagonal matrix is given by 'diag' symbol). It is given as

$$\begin{aligned}\hat{\Pi}(t,t+\Delta t)&=(1-1_{t,t+\Delta t})(\hat{I}_U\times\hat{I}_L)+\\ &1_{t,t+\Delta t}(|0,0,1\rangle_U\langle 0,0,1|_U\times\hat{I}_L)=\\ &(1-1_{t,t+\Delta t})(\hat{I}_U\times\hat{I}_L)+\\ &1_{t,t+\Delta t}(|0,0,1\rangle_U\langle 0,0,1|_U\times(|1,0,0\rangle_L\langle 1,0,0|_L+\\ &|0,1,0\rangle_L\langle 0,1,0|_L+|0,0,1\rangle_L\langle 0,0,1|_L))=\\ &=(1-1_{t,t+\Delta t})\hat{I}_{9\times 9}+1_{t,t+\Delta t}diag(0,0,1)\times\hat{I}_{3\times 3}\\ &=diag((1-1_{t,t+\Delta t}),(1-1_{t,t+\Delta t}),(1-1_{t,t+\Delta t}),\\ &(1-1_{t,t+\Delta t}),(1-1_{t,t+\Delta t}),(1-1_{t,t+\Delta t}),1,1,1)\end{aligned} \quad (20)$$

D. Correlation Function for Classical and Quantum Approaches for Single-Electron Lines

In this work, two capacitively coupled single-electron lines (SEL) are treated by the tight-binding model with the use of three nodes for each line to describe the electron occupancy. It shall be underlined that the most simplistic approach towards the two SELs can be attempted with the use of two nodes for each line. In such a case, it is possible to introduce a correlation function for both quantum and classical treatments of the system under consideration. Let us start from the quantum approach. The Hamiltonian of the system having flat bottoms of potentials can be written as

$$H=\begin{pmatrix}E_{c1}+2E_p & e^{i\beta}t_{s2} & e^{i\alpha}t_{s1} & 0\\ e^{-i\beta}t_{s2} & E_{c2}+2E_p & 0 & e^{i\alpha}t_{s1}\\ e^{-i\alpha}t_{s1} & 0 & E_{c2}+2E_p & e^{i\beta}t_{s2}\\ 0 & e^{-i\alpha}t_{s1} & e^{-i\beta}t_{s2} & E_{c1}+2E_p\end{pmatrix}, \quad (21)$$

where $E_{c1}=\frac{q^2}{d}$ and $E_{c2}=\frac{q^2}{\sqrt{d^2+a^2}}$, so $E_{c1}-E_{c2}=\frac{q^2}{d}-\frac{q^2}{\sqrt{d^2+a^2}}>0$. The hopping terms are parametrized by t_{s1} and t_{s2}. This last Hamiltonian refers to the quantum state describing the occupancy of four nodes at upper U=(1,2) or lower line L=(1',2') by two spatially separated electrons

$$|\psi\rangle=\gamma_1(t)|1\rangle|1'\rangle+\gamma_2(t)|1\rangle|2'\rangle+\gamma_3(t)|2\rangle|1'\rangle+\gamma_4(t)|2\rangle|2'\rangle. \quad (22)$$

Normalization condition requires $|\gamma_1|^2+\cdots+|\gamma_4|^2=1$. We have four eigenenergies

$$\begin{aligned}E_1&=\frac{1}{2}(E_{c1}+E_{c2}+4E_p-\sqrt{(E_{c1}-E_{c2})^2+4(t_{s1}-t_{s2})^2}),\\ E_2&=\frac{1}{2}(E_{c1}+E_{c2}+4E_p+\sqrt{(E_{c1}-E_{c2})^2+4(t_{s1}-t_{s2})^2}),\\ E_3&=\frac{1}{2}(E_{c1}+E_{c2}+4E_p-\sqrt{(E_{c1}-E_{c2})^2+4(t_{s1}+t_{s2})^2}),\\ E_4&=\frac{1}{2}(E_{c1}+E_{c2}+4E_p+\sqrt{(E_{c1}-E_{c2})^2+4(t_{s1}+t_{s2})^2}),\end{aligned} \quad (23)$$

fulfilling $E_1<E_2$, $E_3<E_4$ as corresponding to four eigenenergy states

$$\begin{aligned}|E_1\rangle&=\begin{pmatrix}-e^{i(\alpha+\beta)},\\ -\frac{2e^{i\alpha}(t_{s1}-t_{s2})}{\sqrt{(E_{c1}-E_{c2})^2+4(t_{s1}-t_{s2})^2}-E_{c1}+E_{c2}},\\ \frac{2e^{i\beta}(t_{s1}-t_{s2})}{\sqrt{(E_{c1}-E_{c2})^2+4(t_{s1}-t_{s2})^2}-E_{c1}+E_{c2}},\\ 1\end{pmatrix},\\ |E_2\rangle&=\begin{pmatrix}-e^{i(\alpha+\beta)},\\ \frac{2e^{i\alpha}(t_{s1}-t_{s2})}{\sqrt{(E_{c1}-E_{c2})^2+4(t_{s1}-t_{s2})^2}+E_{c1}-E_{c2}},\\ -\frac{2e^{i\beta}(t_{s1}-t_{s2})}{\sqrt{(E_{c1}-E_{c2})^2+4(t_{s1}-t_{s2})^2}+E_{c1}-E_{c2}},\\ 1\end{pmatrix},\\ |E_3\rangle&=\begin{pmatrix}e^{i(\alpha+\beta)},\\ -\frac{2e^{i\alpha}(t_{s1}+t_{s2})}{\sqrt{(E_{c1}-E_{c2})^2+4(t_{s1}+t_{s2})^2}-E_{c2}+E_{c1}},\\ -\frac{2e^{i\beta}(t_{s1}+t_{s2})}{\sqrt{(E_{c1}-E_{c2})^2+4(t_{s1}+t_{s2})^2}-E_{c2}+E_{c1}},\\ 1\end{pmatrix},\\ |E_4\rangle&=\begin{pmatrix}e^{i(\alpha+\beta)},\\ \frac{2e^{i\alpha}(t_{s1}+t_{s2})}{\sqrt{(E_{c1}-E_{c2})^2+4(t_{s1}+t_{s2})^2}+E_{c1}-E_{c2}},\\ \frac{2e^{i\beta}(t_{s1}+t_{s2})}{\sqrt{(E_{c1}-E_{c2})^2+4t_{s1}+t_{s2})^2}+E_{c1}-E_{c2}},\\ 1\end{pmatrix}.\end{aligned} \quad (24)$$

with ground state

$$E_3=E_g=\frac{1}{2}(E_{c1}+E_{c2}+4E_p-\sqrt{(E_{c1}-E_{c2})^2+4(t_{s1}+t_{s2})^2}). \quad (25)$$

We observe that in the ground state, the probability of occurrence of two particles at the maximum distance $p_{1,2'}=p_{2,1'}=$

$p_{anticorr}$ to their probability of occurrence at the minimum distance $p_{1,1'} = p_{2,2'} = p_{corr}$ is given by the formula:

$$\frac{p_{acorr}}{p_{corr}} = \left[\frac{\sqrt{(E_{c1}-E_{c2})^2+4(t_{s1}+t_{s2})^2}-(E_{c1}-E_{c2})}{2(t_{s1}+t_{s2})}\right]^2 = \left[\frac{\sqrt{q^2(\sqrt{d^2+(a+b)^2}-d)^2+4(t_{s1}+t_{s2})^2}}{2(t_{s1}+t_{s2})d\sqrt{d^2+(a+b)^2}} - \frac{q^2(\sqrt{d^2+(a+b)^2}-d)}{2(t_{s1}+t_{s2})d\sqrt{d^2+(a+b)^2}}\right]^2 \quad (26)$$

It is worth mentioning that the ground state of two coupled SELs brings electrons partly into the anticorrelated position (the two electrons at the maximum distance) and the correlated positions (the two electrons at the minimum distance), which simply means that the anticorrelation is not greatly pronounced in the quantum case at it is the case of the classical picture. One can refer to the following dependence of the ratio between probabilities for the state to be anticorrelated or correlated, as depicted by Fig. 5.

The quantum state in case of time-independent Hamiltonian can be expressed as

$$|\psi\rangle = \sqrt{p_{E1}}e^{\phi_{E10}i}e^{\frac{1}{\hbar i}E_1 t}|E_1\rangle + \sqrt{p_{E2}}e^{\phi_{E20}i}e^{\frac{1}{\hbar i}E_2 t}|E_2\rangle + \sqrt{p_{E3}}e^{\phi_{E30}i}e^{\frac{1}{\hbar i}E_3 t}|E_3\rangle + \sqrt{p_{E4}}e^{\phi_{E40}i}e^{\frac{1}{\hbar i}E_4 t}|E_4\rangle \quad . \quad (27)$$

Having $E_{c1} = \frac{q^2}{d}$ and $E_{c2} = \frac{q^2}{\sqrt{d^2+a^2}}$ so $E_{c1} - E_{c2} = \frac{q^2}{d} - \frac{q^2}{\sqrt{d^2+a^2}} > 0$ and hopping terms t_{s1}, t_{s2} we obtain Hamiltonian and a correlation function C.

We refer to the physical situation depicted in Fig. 6 and utilize the correlation function C to capture as to what extent the two electrons are in a correlated state being both either on the left or on the right side that is corresponding to terms $N_{-,-}, N_{+,+}$, or in an anticorrelated state (expressed by terms $N_{+,-}$ and $N_{-,+}$). Such function is commonly used in spin systems and is a measure of non-classical correlations. Using a tight-binding model describing two electrostatically coupled SELs and using the same correlation function applicable in the test of Bell theory of entangled spins [15], we obtain the correlation function C given by formula:

$$C = \frac{N_{+,+}+N_{-,-}-N_{-,+}-N_{+,-}}{N_{+,+}+N_{-,-}+N_{-,+}+N_{+,-}} = 4\Big[\frac{\sqrt{p_{E1}}\sqrt{p_{E2}}(t_{s1}-t_{s2})\cos[-t\sqrt{(E_{c1}-E_{c2})^2+4(t_{s1}-t_{s2})^2}+\phi_{E10}-\phi_{E20}]}{\sqrt{(E_{c1}-E_{c2})^2+4(t_{s1}-t_{s2})^2}} + \frac{\sqrt{p_{E3}}\sqrt{p_{E4}}(t_{s1}+t_{s2})\cos[-t\sqrt{(E_{c1}-E_{c2})^2+4(t_{s1}+t_{s2})^2}+\phi_{E30}-\phi_{E40}]}{\sqrt{(E_{c1}-E_{c2})^2+4(t_{s1}+t_{s2})^2}}\Big] - (E_{c1}-E_{c2})\Big[\frac{p_{E1}-p_{E2}}{\sqrt{(E_{c1}-E_{c2})^2+4(t_{s1}-t_{s2})^2}} + \frac{p_{E3}-p_{E4}}{\sqrt{(E_{c1}-E_{c2})^2+4(t_{s1}+t_{s2})^2}}\Big] \quad (28)$$

Classical intuition points out that when the kinetic energy of electrons goes to zero they shall be anticorrelated due to the presence of the repulsive Coulomb force. On the other hand, when the kinetic energy is dominant, the Coulomb interaction does not matter so much and the correlation function shall be zero or positive. Four fundamental solutions for the correlation function corresponding to the occupancy of four eigenenergies are given by Fig. 7. Indeed, when only the ground state is occupied so $p_1 = 1$, then $C < 1$, as depicted in Fig. 8. It is remarkable to observe that $C = 0$ if $p_1 = p_3 = 0.5$. We also observe that if the two qubits are electrostatically decoupled then $C = 0$ does not need to apply. However, for certain cases, the weaker the Coulomb interaction the sharper the peaks in the 2-SEL correlation function C, as depicted by Fig.8.

Now we turn towards the classical description of the two coupled single-electron lines using Newtonian dynamics as we expect qualitative changes in the correlation function due to the unique differences between the quantum and classical pictures. The confinement potential is approximated as a step function and presence of Poyting vector is neglected in the space as Hamiltonian system is time-independent, and system Hamiltonian corresponds to the classical mechanical energy that is preserved if we omit radiation emission for two particles subjected to acceleration and deceleration during different moments of motion that can be periodic or aperiodic. We have

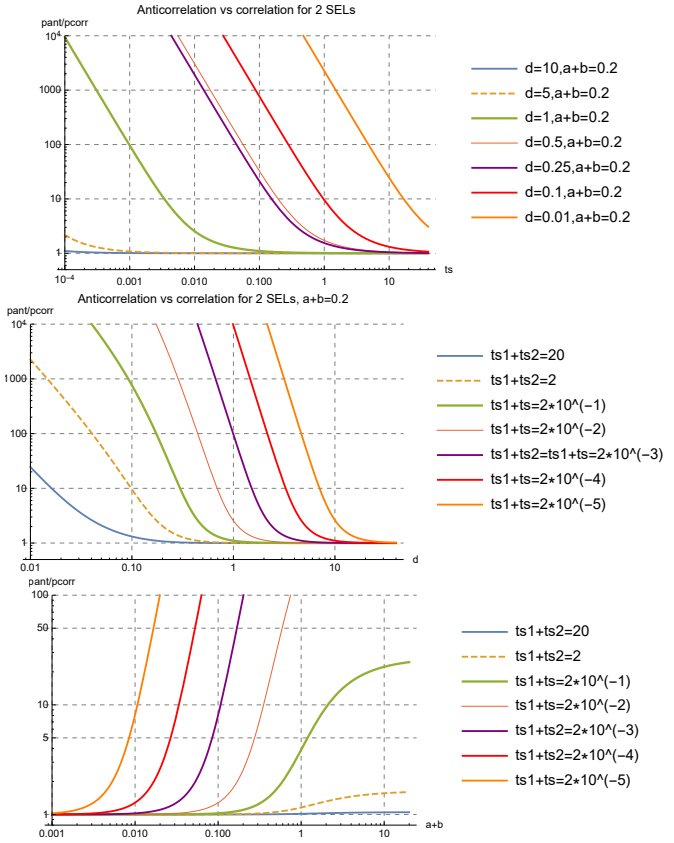

Fig. 5. The ratio of probabilities in 2 SELs ground state between correlated and anticorrelated quantum state components is very strongly depending on hopping constants by term $t_{s1} + t_{s2}$ and very strongly depends on size of quantum wells denoted by a and distance between two two neighbours b.

the minimalistic classical Hamiltonian for 2SELs given as

$$\hat{H} = \frac{1}{2m_1}p_1(t)^2 + \frac{1}{2m_2}p_2(t)^2 + \frac{q^2}{\sqrt{d^2 + (x_1(t) - x_2(t))^2}} + V_0\Theta(x_1(t) - x_{max1}) + V_0\Theta(-x_1(t) - x_{max1}) + V_0\Theta(x_2(t) - x_{max2}) + V_0\Theta(-x_2(t) - x_{max2}) + V_{b1}\Theta(x_1(t) - x_{b1}) + V_{b1}\Theta(-x_1(t) - x_{b1}) + V_{b2}\Theta(x_2(t) - x_{b2}) + V_{b2}\Theta(-x_2(t) - x_{b2}). \quad (29)$$

We simplify the situation by having two symmetric masses $m_1 = m_2 = m$ and same charges q, and having $x_{max1} = x_{max2} = x_{max}$. We set $x_{b1} = x_{b2} \to 0$. There are always two possible grounds states of the classically interacting electrons in 2 SELs configuration corresponding to the same energy when charged particles of same charge are confined in local potential that corresponds to two positions of particle that are at maximum distance $x_2(t) = \mp x_{min} = constans, \frac{dx_1}{dt}(t) = 0, \frac{d^2x_1}{dt^2}(t) = 0, x_2(t) = \pm x_{min}, \frac{dx_1}{dt}(t) = 0, \frac{d^2x_1}{dt^2}(t) = 0$. Classical ground state is maximally anticorrelated. On the contrary the same situation in quantum picture has only one ground state and this state is not maximally anticorrelated and is partly correlated what is expressed by formula 26. Moreover, in the classical picture of 2 SELs, one can observe the emergence of deterministic chaos that is heavily pronounced in the classical system, as depicted in Figs. 10–11. Now we are moving towards a description of classical 2-SEL system in case of perfect correlated or anticorrelated electrons. From the classical Hamiltonian we determine the equations of motion of the two electrons assuming the existence of the antisymmetric case $\pm x(t) = x_1(t) = -x_2(t)$ at all instances of motion for the system symmetric around $x = 0$. We assume that the distance between electrons $\sqrt{d^2 + x(t)^2} \approx d$. We have

$$mv^2(t) + \frac{q^2}{\sqrt{d^2 + x^2}} = E_c > 0, \frac{d^2x}{dt} = \frac{xq^2}{(\sqrt{d^2 + x^2})^3}.$$

In simplified case $d \gg x$ and thus we can write

$$m\frac{d^2x(t)}{dt^2} = x\frac{q^2}{d^{\frac{3}{2}}}. \quad (30)$$

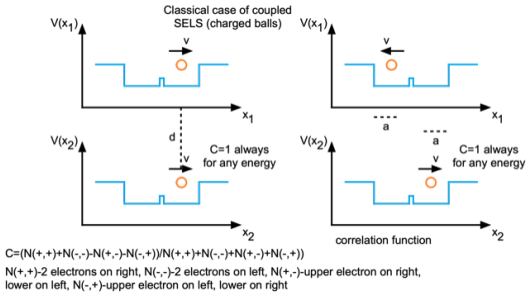

Fig. 6. Case of electrostatically coupled charged particles confined by local potentials and electrostatically interacting. Concept of correlation/anticorrelation in their positions.

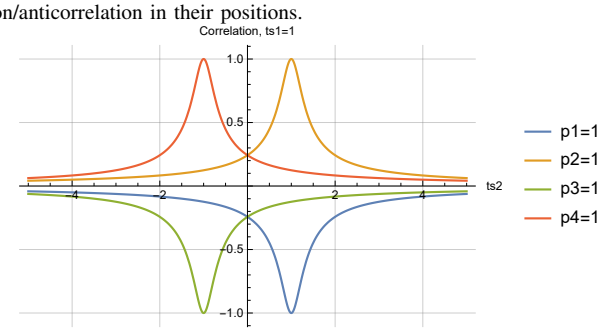

Fig. 7. Four main fundamental configurations named as anticorrelation and correlation for system of coupled SEL depicted in Fig. 6. The correlation function C that are grasped by formula (28) corresponding to the full occupancy of one among four eigenenergies.

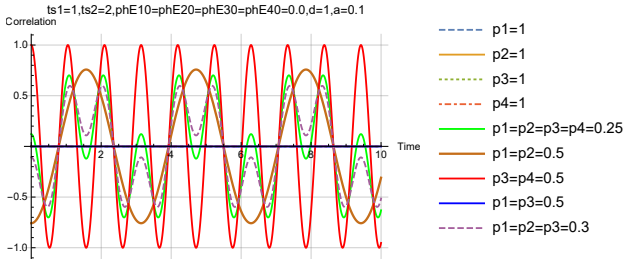

Fig. 8. Correlation function C with time for time-independent Hamiltonian corresponding to full and partial occupancy of 4 eigenenergies of 2-SEL system.

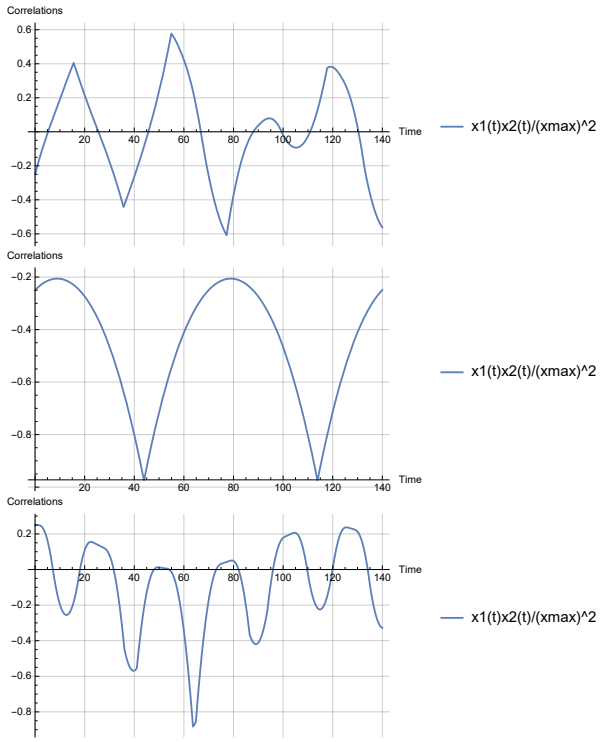

Fig. 9. Varying dependence of classical correlation function [$C = \frac{x_1(t)x_2(t)}{x^2_{max}}$] over time. Upper case refers to 2-SELs with particles of significantly different speeds at anticorrelated positions at initial time; middle figure describes two perfectly anticorrelated particles (VII); third case refers to the proceeding figure 10.

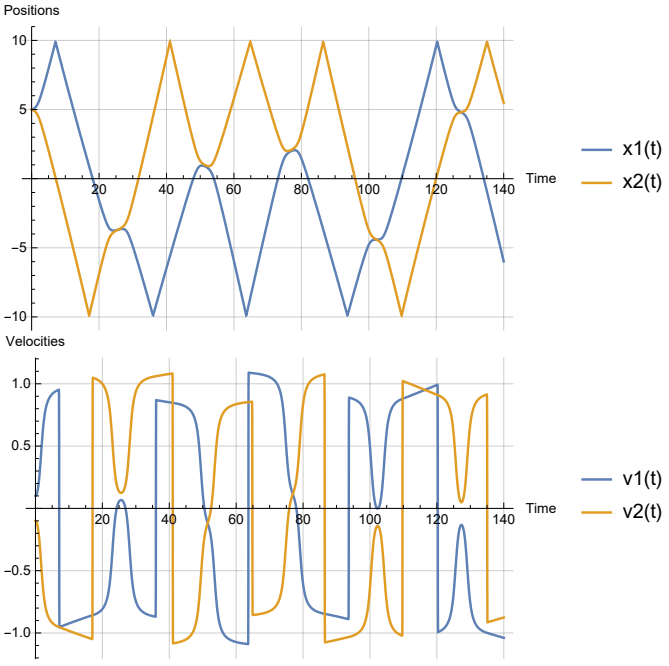

Fig. 10. Evolution of positions $x_i(t)$ and velocities $v_i(t)$ for the system of 2 electrostatically coupled SELs in classical picture.

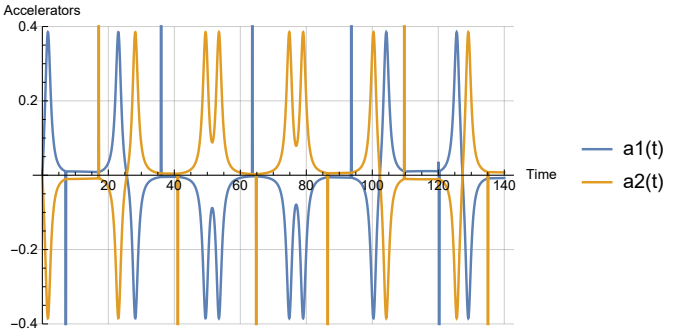

Fig. 11. Acceleration for the system of 2 coupled oscillators from Fig.10 confined by local potential with coordinates $x_1, x_2 \in (-x_{max}, x_{max})$ with $x_{max} = 10$.

and it has solutions for each electron position

$$x(t) = \frac{\sqrt{m}v_0 d^{3/4}}{q} \sinh(\frac{q}{\sqrt{m}d^{3/4}}t). \tag{31}$$

We notice that $x_{max} = \frac{\sqrt{m}v_0 d^{3/4}}{q} sinh(\frac{q}{\sqrt{m}d^{3/4}}\frac{T}{4})$ and the period of oscillations is

$$T = 4\frac{\sqrt{m}d^{3/4}}{q} Arc_{\sinh}(\frac{qx_{max}}{\sqrt{m}v_0 d^{3/4}}) \tag{32}$$

if $x_1(t=0) = x_2(t=0) = 0$ and when $\frac{dx_1}{dt}(t=0) = -\frac{x_2}{dt}(t=0) = v_0 \neq 0$, which is a definition of perfect anticorrelation. Collision with walls is occurring at $\frac{T}{4}$ time while the total size of classical well is $2x_{max}$. We observe that $x_1(t) = \frac{\sqrt{m}v_0 d^{3/4}}{q} \sinh(\frac{q}{\sqrt{m}d^{3/4}}t) = -x_2(t)$ for $t \in [0, \frac{T}{4}]$. Correlation function C is given analytically

$$C(t) = -\frac{1}{x^2_{max}} \frac{mv_0^2 d^{3/2}}{q^2} (\sinh(\frac{q}{\sqrt{m}d^{3/4}}t))^2 < 0 \tag{33}$$

and is negative for any energy E_c (function of q, d, v_0) of the system. Such situation occurs only in some subsets of the classical case since in the quantum case the sign of function C depends on the occupancy of the energetic levels. In the classical treatment of 2-SELs there exist the case of perfectly correlated electrons at any distance that is independent on the system energy if we are above the ground state.

It is possible to specify such situation when at $t = 0$ we have $x_1(t=0) = x_2(t=0) = 0$ and when $\frac{dx_1}{dt}(t=0) = \frac{x_2}{dt}(t=0) = v_0$. In such a case, the Coulomb force will act perpendicular to the direction of motion and will play no role in the electron movement. Electron movement will be correlated and with constant speed over time, with periodic reflections from the potential walls. The correlation function will have the form

$$C(t) = \frac{1}{x^2_{max}} (v_0)^2 t^2 \tag{34}$$

within time $t \in [0, T/4]$. A perfect correlation of electrons in the classical situation can occur for any energy (if kinetic energy is larger than zero) of the system $E_c > 0$. It is one of the key differences from the quantum situation when the

positive value of correlation function can occur only for certain system eigenenergies as given by formula (28).

It shall be underlined that the perfectly correlated electrons generate higher overall magnetic field energy as it is the case of two electric currents of the same sign (correlated electron movement in one direction) generated by each electron. In the case of anticorrelated electrons we are dealing with electric currents of opposite sign that are generating magnetic field in the opposite directions, thus decreasing the overall magnetic field. Therefore, thermal equilibrium of 2-SEL will favor anticorrelation of two electrons. It shall be underlined that, in accordance with the classical thermodynamics that applies to the case of two electrons treated classically, the movement of electron with certain acceleration will cause the occurrence of non-zero Poynting vector into the space and thus electron's energy will be emitted in the form of electromagnetic radiation. In such way one can introduce effective dissipative term to the movement of electrons and it will cause the system mechanical energy to eventually vanish. After sufficiently long time the electrons will stop their oscillatory movement and they will move into ground state that is perfectly anticorrelated and corresponds to the case when $x_2 = x_1 = \pm x_{max}$ and $\frac{d}{dt}x_1 = \frac{d}{dt}x_2$ and when $\frac{d^2}{dt^2}x_1 = 0 = \frac{d^2}{dt^2}x_2 = 0$. It is also worth mentioning that the ground state of two classical electrons in 2-SELs is different from the quantum ground state of 2-SELs.

There exists the case of two perfectly anticorrelated electrons at any distance in the classical treatment that is independent of the system energy. Such situation does not take place in the quantum case as treated by the tight-binding model given by formula (28) that has discrete spectra of energies as specified by (23).

We can write the equations of motion of two electrons assuming the existence of antisymmetric case $x_1(t) = -x_2(t)$ at all instances of motion for the system symmetric around $x = 0$. From the equation

$$mv^2(t) + \frac{q^2}{\sqrt{d^2 + 4x(t)^2}} = E_c = \text{const} > 0,$$

we obtain the equation $\sqrt{\frac{q^4}{(E_c - mv^2(t))^2} - d^2} = 2x(t)$ and consequently we obtain the equation of motion

$$m\frac{dv}{dt} = \frac{1}{2}\sqrt{\frac{q^4}{(E_c - mv^2(t))^2} - d^2} \cdot q^2 (E_c - mv^2(t))^3 \frac{1}{q^6} = \frac{1}{2q^4}\sqrt{q^4(E_c - mv^2(t))^4 - d^2(E_c - mv^2(t))^6}. \quad (35)$$

Finally we obtain the equation

$$\frac{dv}{\sqrt{q^4(E_c - mv^2(t))^4 - d^2(E_c - mv^2(t))^6}} = dt\frac{1}{2mq^4} \quad (36)$$

We introduce a new variable $u = \frac{d}{q}(E_c - mv^2)$. We have $du = -2\frac{md}{q}vdv$. We also notice that $\sqrt{(\frac{E_c}{m} - \frac{q}{md}u)} = v$. The last expressions imply

$$dv = -\frac{q}{2md}\frac{du}{v} = -\frac{q}{2md}\frac{du}{\sqrt{(\frac{E_c}{m} - \frac{q}{md}u)}} = -\frac{\sqrt{q}}{2\sqrt{md}}\frac{du}{\sqrt{(\frac{E_c d}{q} - u)}}. \quad (37)$$

The last expression allows us to write integral

$$\int \frac{dv}{\sqrt{q^4(E_c - mv^2))^4 - d^2(E_c - mv^2)^6}} = \frac{d^2}{q^4}\int \frac{du}{\sqrt{(\frac{E_c d}{q} - u)}}\frac{1}{u^2\sqrt{1-u^2}} = s_1 \int \frac{du}{\sqrt{(s-u)}}\frac{1}{u^2\sqrt{1-u^2}}. \quad (38)$$

Setting $s_1 = \frac{d^2}{q^4}$ and $s = \frac{E_c d}{q}$ we obtain the integral $s_1 \int \frac{du}{\sqrt{(s-u)}}\frac{1}{u^2\sqrt{1-u^2}}$ that has a solution as three types of elliptic functions given in Appendix VII.

E. Classical Weak Measurement on 2-SEL System

Measurement on a given physical system is about introducing an interaction of it with an external physical system that acts as a probe. If this interaction is strong (weak) we are dealing with a strong (weak) measurement. We shall introduce an external charged particle at a certain distance that can move only in parallel to the system being probed and then we apply Newtonian equations of motion. For the sake of simplicity, we consider only interaction of the probe that is moving electron across one line with nearest charged particle, as depicted in Fig. 14. At a first level of approximation, the movement of external electron is the perturbation to the physical system of two electrons (2-SELs).

F. Weak Quantum Measurement on 2-SEL System

We consider an interaction of two single-electron lines (2-SEL) that incorporate qubits A and B with an external line along which there is a movement of position-based qubit C. The CMOS structures have the capability to impose a constrained 'movement' of a virtual qubit along single-electron lines. This way, the moving qubit becomes effectively a flying qubit, which is a term usually reserved for polarized photons participating in quantum information processing. At a very far distance, there is no interaction between the flying qubit and 2-SELs. In such a case one can have a tensor of two density matrices being a density matrix of 2-SELs denoted by ρ_{AB} and the external flying qubit. We have a three-body quantum density matrix given as

$$\hat{\rho}_{ABC} = \hat{\rho}_C \times \hat{\rho}_{AB} = \begin{pmatrix} \rho_C[1,1]\hat{\rho}_{AB} & \rho_C[1,2]\rho_{AB} \\ \rho_C[2,1]\hat{\rho}_{AB} & \rho_C[2,2]\rho_{AB} \end{pmatrix} = \begin{pmatrix} \hat{A}_1 & \hat{B}_1 \\ \hat{C}_1 & \hat{D}_1 \end{pmatrix}. \quad (39)$$

We immediately recognize that we can obtain the density matrix of particle C by tracing out the existence of density matrix AB

$$\hat{\rho}_C = \sum_{i_A=\{1,2\}, j_B=\{1',2'\}} \langle i_A, j_B | \, \hat{\rho}_{ABC} \, | i_A, j_B \rangle \, . \tag{40}$$

In similar way we obtain the density matrix for 2-SEL system

$$\hat{\rho}_{AB} = \sum_{k_C=\{1,2\}} \langle k_C | \, \hat{\rho}_{ABC} \, | k_C \rangle \, . \tag{41}$$

The last expressions can be expressed by formula

$$\hat{\rho}_C = \begin{pmatrix} Tr(\hat{A}_1) & Tr(\hat{B}_1) \\ Tr(\hat{C}_1) & Tr(\hat{D}_1) \end{pmatrix}, \hat{\rho}_{AB} = \hat{A}_1 + \hat{D}_1. \tag{42}$$

System of 2-SELs with the flying qubit can be reagarded as non-dissipative system and thus one can write the following equations of motion

$$\rho(t) = e^{\frac{1}{-i\hbar} H_0 t} e^{\frac{1}{i\hbar} \int_0^t \hat{H}(t')dt'} \rho(t) e^{\frac{1}{-i\hbar} \int_0^t \hat{H}(t')dt'} e^{\frac{1}{-i\hbar} H_0 t}, \tag{43}$$

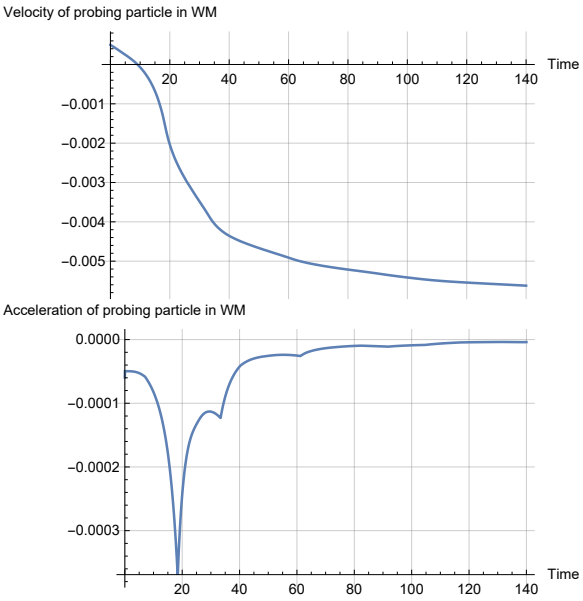

Fig. 12. Case of the classical measurement with electron used for probing of 2-SELs.

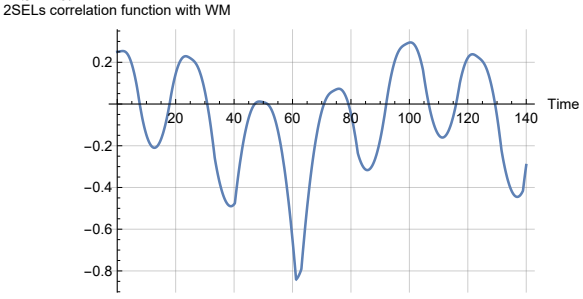

Fig. 13. Correlation function for 2-SELs under classical weak measurement from external probing charged particle. One shall refer to the bottom plot of Fig. 9 and to Fig.14.

where H_0 is a time-independent Hamiltonian of isolated 2-SELs and isolated external qubit, while $H(t')$ stands for electrostatic interaction between the flying qubit and 2-SELs. We have the total system Hamiltonian having time-independent and time-dependent components

$$\hat{H}(t) = \hat{H}_0 + \hat{H}_1(t) = \\ = (\hat{I}_C \times \hat{H}_{AB} + \hat{H}_C \times \hat{I}_{AB})_0 + \hat{H}_{AC}(t) \times \hat{I}_B, \tag{44}$$

where $\hat{I}_{AB}$ and $\hat{I}_C$ are identity matrices acting on the 2-SELs and flying qubit, while $\hat{H}_{AB}$ is 2-SEL Hamiltonian. $\hat{H}_C$ is the flying qubit Hamiltonian and $\hat{H}_{AC}(t)$ is the interaction Hamiltonian between A line and flying qubit C (note: for the sake of simplicity we neglect the interaction between B line and C qubit). The detailed structure of those Hamiltonians are given in Appendix C.

Defining 2-SEL correlation function previously defined by formula (28), so $C = C_{AB}$, incorporated into three-body system takes form as $C_{AB,C} = \hat{I}_C \times \hat{C}_{AB}$ and, consequently, we obtain the following time dependence of correlation function given as

$$C(t) = Tr(C_{AB,C} \rho(t)). \tag{45}$$

Details of the calculations can be found in Appendix C. Finally, we obtain the formula for correlation function of the

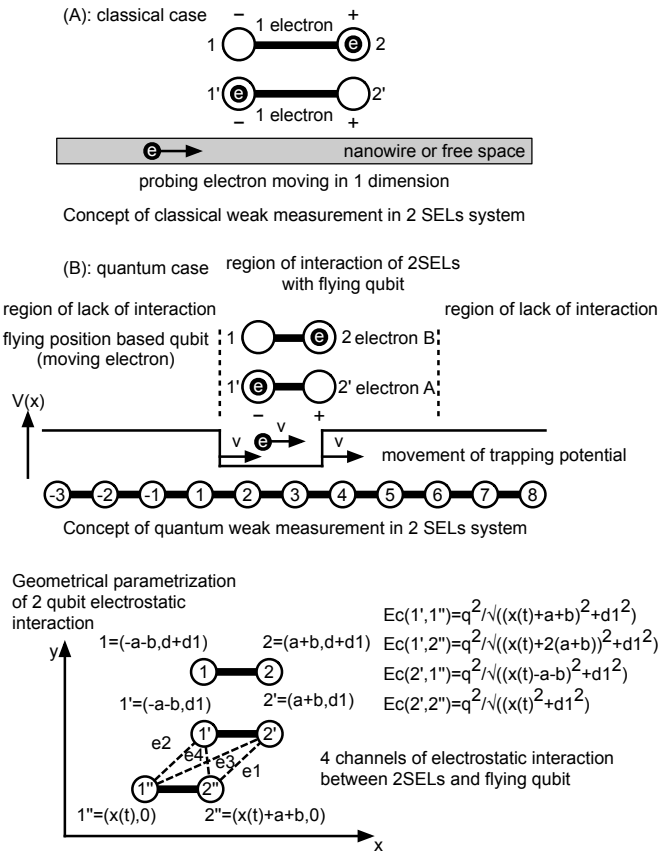

Fig. 14. Concept of classical and quantum weak measurements in a double single-electron line system. All simulations were conducted for the classical case.

2-SEL system interacting weakly with the flying qubit in the form as

$$C(t)=\frac{(E_{c1}-E_{c2})^2-4\cos\left(\frac{t\sqrt{(E_{c1}-E_{c2})^2+16}}{\hbar}\right)\left(\cos\left(\int_0^t dt'\frac{E_{c11''}(t')-E_{c1''2}(t')}{\hbar}\right)+\cos\left(\int_0^t dt'\frac{E_{c2''1}(t')-E_{c2pp2}(t')}{\hbar}\right)-2\right)}{(E_{c1}-E_{c2})^2+16}$$
$$+\frac{4\cos\left(\int_0^t dt'\frac{E_{c11''}(t')-E_{c1''2}(t')}{\hbar}\right)+4\cos\left(\int_0^t dt'\frac{E_{c2''1}(t')-E_{c2''2}(t')}{\hbar}\right)+8}{(E_{c1}-E_{c2})^2+16} \quad (46)$$

where $E_{c11''}(t)=\frac{q^2}{\sqrt{(x(t)+a+b)^2+d_1^2}}$,
$E_{c12''}(t)=\frac{q^2}{\sqrt{(x(t)+2(a+b))^2+d_1^2}}$,
$E_{c21''}(t)=\frac{q^2}{\sqrt{(x(t)-(a+b))^2+d_1^2}}$,
$E_{c22''}(t)=\frac{q^2}{\sqrt{(x(t))^2+d_1^2}}$.
The movement of the flying qubit can be described, for example, by a constat velocity $v=v_0$, so $x(t)=x_0+v_0t$. In case of a time-dependent flying qubit, $x(t)=x(t_0)+\int_{t_0}^t v_f(t')dt'$, where $v_f(t)$ is an instantaneous speed of the flying qubit. The only assumption for this model is that particle at time $t=0$ is at a far distance from 2-SELs.

G. Analogies of Coupled SELs with Other Physical Systems

The repulsion (anticorrelation in position) of two electrons occurs in two parallel SELs and can be used in the construction of quantum SWAP gate. Therefore, the results obtained analytically and numerically on the two interacting SELs has its meaning in the development of quantum technologies [10] and also point to the interlink between the fundamental and applied science. It is important to underline that the tight-binding model allows for a quick detection of entangled states and for a transfer of this information into Schrödinger formalism, which has its importance in the design of quantum computer consisting of many coupled entangled qubits (fundamental modelling due to the large Hilbert space is limited to 10 qubits). Quite obviously, the Schrödinger equation gives detailed space resolution of quantum mechanical phenomena taking place in 2 or N electrostatically coupled SELs that might contain an arbitrary number of quantum wells. Incorporation of spin effects is also possible in the given framework, but is beyond the scope of this work. The tight-binding model can be derived from the Schrödinger formalism (and vice versa) and is the simplistic version of the Hubbard model that is a very universal model capable of descring various collective phenomena in condensed matter physics. Therefore, it is expected that the tight-binding model can be also effective in describing physical effects in various programmable (electrostatically controlled) CMOS nanostructures. It shall be also underlined that the described position-dependent qubits are analogical to superconducting Cooper pair boxes where quantum phase transitions have been observed [6], [12]. The hopping term in the tight-binding model of semiconductor position-dependent qubits is analogical to energy of Josephson coupling in superconducting Cooper pair box (or in other types of superconducting qubits). Therefore, the existence of quantum phase transitions [13] is expected to occur in the studied SELs system since quantum phase transitions occurs in arrays of electrostatically coupled Josephson junctions. Therefore one is expecting to spot quantum phase transition in SELs coupled to superconducting Cooper pair boxes.

IV. Conclusion

Described two single-electron lines (SEL) are approximated by occupancy of two electrons at three different nodes spread out on each line: 1(1'), 2(2') and 3(3'), as depicted in Fig. 1. In such a way, two electrostatic semiconductor position-based qubits can be characterized by what makes the result of this work valid for the case of two capacitively interacting semiconductor qudits or qubits [2]. In the presented work, new qualitative features of two capacitively coupled single-electron lines were described as occupancy oscillations at SEL nodes depicted in Fig. 4. Obtained occupancy oscillations have different form in the classically coupled electrical lines. Particular difference between quantum and classical description of two SELs is reflected in the anticorrelation principle applicable to the electrons' positions. Electrons tend to have maximum distanced due to the electrostatic repulsion. This anticorrelation principle is less pronounced in the quantum ground state than in the classical ground state of two coupled SELs (2-SEL). In the classical picture in 2-SEL system, electrons take such positions that their distance is maximimzed and kinetic energy is zero. However in the quantum case of 2-SELs, kinetic energy of electrons is never zero, which stands for fundamental difference between the classical and quantum pictures. Moreover, the entanglement is present in the quantum ground state of 2-SELs, which is not present in the classical 2-SELs. In the conducted work, the correlation function was introduced and this function weight the degree of correlation and anticorrelation in 2-SEL system. Quite clearly, the presence of anticorrelation and correlation in the 2-SEL ground state is the indication of quantumness of the studied structure. What is more, there are two configurations for electrons corresponding to the classical ground state of 2-SELs while there is only one quantum ground state of 2-SELs. It is also quite interesting to observe the physical change of the 2-SEL system during

the classical and quantum weak measurement with the use of external electron as a probe. In the classical case, the moving electron constrained to 1D, as it is the case of nanowire, is changing its momentum and perturbing the 2-SEL state. On another hand, in the quantum treatment of 2-SEL system, it is recommendable to use a flying position based qubit as the probe moving in 1D chain of coupled quantum dots. In such a case, one is changing the physical state of the flying qubit while perturbing the state of the 2-SELs system. Anticorrelation function is monitored during this process and analytical formula was specified. From the obtained solutions, we can spot the possible transitions between energy levels (depicted in Fig. 3 as a function of distance between SELs) when the system is subjected to the external microwave field as coming from RF sources placed in the proximity of SELs that can be a factor controlling physical state of coupled SELs. Moreover, the entangled eigenstates were obtained as analytical solutions of simplified system matrix Hamiltonian $\hat{H}$, equation (13), and are given by formulas (48)–(50) in Appendix VI. The entangled states correspond to eigenenergies obtained analytically and given by formulas (14) and depend on SEL distance as expressed by Fig. 3. The conducted study has its relevance in single-electron transistor structures as deriving from nanoscale CMOS. Such systems are expected to mimic various types of programmable quantum matter that can simulate many types of physical phenomena as E_p and t parameters of tight-binding model can be controlled electrostatically in single-electron transistors. One of the interesting illustrations of this is the imitation of metal-insulator phase transition in coupled nanowires, as given in Fig. 3 which can be obtained with electrical tuning of the 2-SELs system.

V. Acknowledgement

We would like to thank to Andrew Mitchell from University College Dublin, Imran Bashir from Equal1, Adam Bednorz from University of Warsaw and to Amir Bozorg from University College Dublin for fruitful discussions and remarks. The assistance for graphical pictures was done by Erik Staszewski (UCD). This work was supported by Science Foundation Ireland under Grant 14/RP/I2921.

VI. Appendix A

The simplified Hamiltonian, given by equation (13) for two electrostatically interacting single-electron lines (Fig. 1) has eigevalues pointed by formulas (10)–(12) and has following eigenvectors

$$\hat{H}_r = \begin{pmatrix} q_{1_1} & 1 & 0 & 1 & 0 & 0 & 0 & 0 & 0 \\ 1 & q_{1_2} & 1 & 0 & 1 & 0 & 0 & 0 & 0 \\ 0 & 1 & q_{1_3} & 0 & 0 & 1 & 0 & 0 & 0 \\ 1 & 0 & 0 & q_{1_2} & 1 & 0 & 1 & 0 & 0 \\ 0 & 1 & 0 & 1 & q_{1_1} & 1 & 0 & 1 & 0 \\ 0 & 0 & 1 & 0 & 1 & q_{1_2} & 0 & 0 & 1 \\ 0 & 0 & 0 & 1 & 0 & 0 & q_{1_3} & 1 & 0 \\ 0 & 0 & 0 & 0 & 1 & 0 & 1 & q_{1_2} & 1 \\ 0 & 0 & 0 & 0 & 0 & 1 & 0 & 1 & q_{1_1} \end{pmatrix}, \quad (47)$$

$$|E_1\rangle = \begin{pmatrix} 1, \\ 0, \\ 0, \\ 0, \\ -1, \\ 0, \\ 0, \\ 0, \\ 1 \end{pmatrix}, |E_2\rangle = \begin{pmatrix} 0, \\ 1, \\ 0, \\ -1, \\ 0, \\ -1, \\ 0, \\ 1, \\ 0 \end{pmatrix},$$

$$|E_{3(4)}\rangle = \begin{pmatrix} -1, \\ \frac{1}{4}(q_{1_1} - q_{1_2} \pm \sqrt{8 + (q_{1_1} - q_{1_2})^2}), \\ 0, \\ \frac{1}{4}(q_{1_1} - q_{1_2} \pm \sqrt{8 + (q_{1_1} - q_{1_2})^2}), \\ 0, \\ -\frac{1}{4}(q_{1_1} - q_{1_2} \pm \sqrt{8 + (q_{1_1} - q_{1_2})^2}), \\ 0, \\ -\frac{1}{4}(q_{1_1} - q_{1_2} \pm \sqrt{8 + (q_{1_1} - q_{1_2})^2}), \\ 1 \end{pmatrix}, \quad (48)$$

$$|E_{5(6)}\rangle = \begin{pmatrix} -1, \\ \frac{1}{4}(q_{1_2} - q_{1_3} \pm \sqrt{8 + (q_{1_2} - q_{1_3})^2}), \\ 0, \\ \frac{1}{4}(q_{1_2} - q_{1_3} \pm \sqrt{8 + (q_{1_2} - q_{1_3})^2}), \\ 0, \\ -\frac{1}{4}(q_{1_2} - q_{1_3} \pm \sqrt{8 + (q_{1_2} - q_{1_3})^2}), \\ 0, \\ -\frac{1}{4}(q_{1_2} - q_{1_3} \pm \sqrt{8 + (q_{1_2} - q_{1_3})^2}), \\ 1 \end{pmatrix}, \quad (49)$$

$$\left|E_{k=(7..9)}\right\rangle =$$

$$\begin{pmatrix} 1, \\ (E_{k=(7..9)}-q_{1_1})/2, \\ \frac{(-E_{k=(7..9)}+q_{1_1})(-2+E^2_{k=(7..9)}+q_{1_1}q_{1_2}-E_{k=(7..9)}(q_{1_1}+q_{1_2}))}{2(-3E_{k=(7..9)}+q_{1_1}+2q_{1_3})}, \\ (E_{k=(7..9)}-q_{1_1})/2, \\ 2, \\ (E_{k=(7..9)}-q_{1_1})/2, \\ 2, \\ \frac{(-E_{k=(7..9)}+q1_1)(-2+E^2_{k=(7..9)}+q_{1_1}q_{1_2}-E_{k=(7..9)}(q_{1_1}+q_{1_2}))}{2(-3E_{k=(7..9)}+q_{1_1}+2q_{1_3})} \end{pmatrix}. \tag{50}$$

It is important to recognize that in the case of electrons partly or wholly localized at the nodes of 2-SEL system, such that all hoping constants $t_{s1,kl}$ and $t_{s2,r'u'}$ are zero, we have no quantum entanglement between 2-SELs if it populates one energetic level and its Hamiltonian becomes diagonal. It brings the following energy eigenstates:

$$|E_1\rangle = \begin{pmatrix} 1 \\ 0 \\ 0 \\ 0 \\ 0 \\ 0 \\ 0 \\ 0 \\ 0 \end{pmatrix}, .. |E_9\rangle = \begin{pmatrix} 0 \\ 0 \\ 0 \\ 0 \\ 0 \\ 0 \\ 0 \\ 0 \\ 1 \end{pmatrix}, \tag{51}$$

and Hamiltonian of system simulating two electrostatically charged insulators has the following structure

$$\hat{H} = \begin{pmatrix} q_{1_1} & 0 & 0 & 0 & 0 & 0 & 0 & 0 & 0 \\ 0 & q_{1_2} & 0 & 0 & 0 & 0 & 0 & 0 & 0 \\ 0 & 0 & q_{1_3} & 0 & 0 & 0 & 0 & 0 & 0 \\ 0 & 0 & 0 & q_{1_2} & 0 & 0 & 0 & 0 & 0 \\ 0 & 0 & 0 & 0 & q_{1_1} & 0 & 0 & 0 & 0 \\ 0 & 0 & 0 & 0 & 0 & q_{1_2} & 0 & 0 & 0 \\ 0 & 0 & 0 & 0 & 0 & 0 & q_{1_3} & 0 & 0 \\ 0 & 0 & 0 & 0 & 0 & 0 & 0 & q_{1_2} & 0 \\ 0 & 0 & 0 & 0 & 0 & 0 & 0 & 0 & q_{1_1} \end{pmatrix}, \tag{52}$$

what brings following eigenenergy values

$$E_1 = q_{1_1}, E_2 = q_{1_2}, E_3 = q_{1_3}, E_4 = q_{1_2}, E_5 = q_{1_1}, \\ E_6 = q_{1_2}, E_7 = q_{1_3}, E_8 = q_{1_2}, E_9 = q_{1_1}. \tag{53}$$

VII. Appendix B: Details of Analytical Solution for Case of Coupled SELs

We continue derivation of the equation of motion imposed by classical picture of 2-SELs and from Hamiltonian 29 we obtain the following expression for velocity of interacting particles with positions $x_1(t) = -x_2(t)$ and velocity vs time as

$$\int \frac{dv}{\sqrt{q^4(E_c - mv^2))^4 - d^2(E_c - mv^2)^6}} = \frac{d^2}{q^4}\int \frac{du}{\sqrt{(\frac{E_c d}{q} - u)}}\frac{1}{u^2\sqrt{1-u^2}} = s_1 \int \frac{du}{\sqrt{(s-u)}}\frac{1}{u^2\sqrt{1-u^2}}. \tag{54}$$

Setting $s_1 = \frac{d^2}{q^4}$ and $s = \frac{E_c d}{q}$, we obtain the integral $s_1 \int \frac{du}{\sqrt{(s-u)}}\frac{1}{u^2\sqrt{1-u^2}}$ that has the solution as

$$\begin{aligned}
s_1 \int \frac{du}{\sqrt{(s-u)}}\frac{1}{u^2\sqrt{1-u^2}} &= \frac{s_1}{s\sqrt{1-u^2}}\Bigg[\frac{(u^2-1)\sqrt{s-u}}{u} + \\
&+\frac{i(s-1)\sqrt{s-u}\sqrt{\frac{u-1}{s-1}}\left(\text{Elliptic}_\text{E}\left(i\sinh^{-1}\left(\sqrt{\frac{u-s}{s+1}}\right),\frac{s+1}{s-1}\right) - \text{Elliptic}_\text{F}\left(i\sinh^{-1}\left(\sqrt{\frac{u-s}{s+1}}\right),\frac{s+1}{s-1}\right)\right)}{\sqrt{\frac{u-s}{u+1}}} + \\
&+\frac{is\sqrt{s-u}\sqrt{\frac{u-1}{s-1}}\text{Elliptic}_\text{F}\left(i\sinh^{-1}\left(\sqrt{\frac{u-s}{s+1}}\right),\frac{s+1}{s-1}\right)}{\sqrt{\frac{u-s}{u+1}}} \\
&-\frac{\left(\sqrt{s-1}+\sqrt{s+1}\right)\left(\sqrt{s-1}-\sqrt{s-u}\right)^2\sqrt{\frac{\sqrt{s-1}\left(\sqrt{s+1}-\sqrt{s-u}\right)}{\left(\sqrt{s-1}+\sqrt{s+1}\right)\left(\sqrt{s-1}-\sqrt{s-u}\right)}}\sqrt{\frac{\sqrt{s-1}\left(\sqrt{s-u}+\sqrt{s+1}\right)}{\left(\sqrt{s-1}-\sqrt{s+1}\right)\left(\sqrt{s-u}-\sqrt{s-1}\right)}}}{\sqrt{s}\left(s-\sqrt{s-1}\sqrt{s+1}-1\right)}\times \\
&\times\sqrt{\frac{\sqrt{s-1}\sqrt{s-u}-\sqrt{s+1}\sqrt{s-u}+s-\sqrt{s-1}\sqrt{s+1}-1}{\left(\sqrt{s-1}+\sqrt{s+1}\right)\left(\sqrt{s-1}-\sqrt{s-u}\right)}}\times \\
&\times\Bigg[\left(\sqrt{s-1}+\sqrt{s}\right)\text{Elliptic}_\text{F}\left(\sin^{-1}\left(\sqrt{\frac{\left(\sqrt{s-1}-\sqrt{s+1}\right)\left(\sqrt{s-1}+\sqrt{s-u}\right)}{\left(\sqrt{s-1}+\sqrt{s+1}\right)\left(\sqrt{s-1}-\sqrt{s-u}\right)}}\right),\frac{\left(\sqrt{s-1}+\sqrt{s+1}\right)^2}{\left(\sqrt{s-1}-\sqrt{s+1}\right)^2}\right) \\
&-2\sqrt{s-1}\times \\
&\times\text{Elliptic}_\text{Pi}\Bigg[\frac{\left(\sqrt{s-1}-\sqrt{s}\right)\left(\sqrt{s-1}+\sqrt{s+1}\right)}{\left(\sqrt{s-1}+\sqrt{s}\right)\left(\sqrt{s-1}-\sqrt{s+1}\right)},\sin^{-1}\left(\sqrt{\frac{\left(\sqrt{s-1}-\sqrt{s+1}\right)\left(\sqrt{s-1}+\sqrt{s-u}\right)}{\left(\sqrt{s-1}+\sqrt{s+1}\right)\left(\sqrt{s-1}-\sqrt{s-u}\right)}}\right), \\
&\frac{\left(\sqrt{s-1}+\sqrt{s+1}\right)^2}{\left(\sqrt{s-1}-\sqrt{s+1}\right)^2}\Bigg]\Bigg] \\
&-\frac{\left(\sqrt{s-1}+\sqrt{s+1}\right)\left(\sqrt{s-1}-\sqrt{s-u}\right)^2\sqrt{\frac{\sqrt{s-1}\left(\sqrt{s+1}-\sqrt{s-u}\right)}{\left(\sqrt{s-1}+\sqrt{s+1}\right)\left(\sqrt{s-1}-\sqrt{s-u}\right)}}\sqrt{\frac{\sqrt{s-1}\left(\sqrt{s-u}+\sqrt{s+1}\right)}{\left(\sqrt{s-1}-\sqrt{s+1}\right)\left(\sqrt{s-u}-\sqrt{s-1}\right)}}}{\sqrt{s}\left(-s+\sqrt{s-1}\sqrt{s+1}+1\right)}\times \\
&\times\sqrt{\frac{\sqrt{s-1}\sqrt{s-u}-\sqrt{s+1}\sqrt{s-u}+s-\sqrt{s-1}\sqrt{s+1}-1}{\left(\sqrt{s-1}+\sqrt{s+1}\right)\left(\sqrt{s-1}-\sqrt{s-u}\right)}}\times \\
&\times\Bigg[\left(\sqrt{s-1}-\sqrt{s}\right)\text{Elliptic}_\text{F}\left(\sin^{-1}\left(\sqrt{\frac{\left(\sqrt{s-1}-\sqrt{s+1}\right)\left(\sqrt{s-1}+\sqrt{s-u}\right)}{\left(\sqrt{s-1}+\sqrt{s+1}\right)\left(\sqrt{s-1}-\sqrt{s-u}\right)}}\right),\frac{\left(\sqrt{s-1}+\sqrt{s+1}\right)^2}{\left(\sqrt{s-1}-\sqrt{s+1}\right)^2}\right)\Bigg] \\
&-2\sqrt{s-1}\text{Elliptic}_\text{Pi}\Bigg[\frac{\left(\sqrt{s-1}+\sqrt{s}\right)\left(\sqrt{s-1}+\sqrt{s+1}\right)}{\left(\sqrt{s-1}-\sqrt{s}\right)\left(\sqrt{s-1}-\sqrt{s+1}\right)}, \\
&\sin^{-1}\left(\sqrt{\frac{\left(\sqrt{s-1}-\sqrt{s+1}\right)\left(\sqrt{s-u}+\sqrt{s-1}\right)}{\left(\sqrt{s-1}+\sqrt{s+1}\right)\left(\sqrt{s-1}-\sqrt{s-u}\right)}}\right),\frac{\left(\sqrt{s-1}+\sqrt{s+1}\right)^2}{\left(\sqrt{s-1}-\sqrt{s+1}\right)^2}\Bigg]\Bigg],
\end{aligned} \tag{55}$$

where $\text{Elliptic}_\text{F}[.,.]$ is the elliptic integral of the first kind, $\text{Elliptic}_\text{E}[.,.]$ is the elliptic integral of the second kind and $\text{Elliptic}_\text{Pi}[.,.]$ is the complete elliptic integral of the third kind as in accordance with nomenclature used by Mathematica symbolic software [14].

VIII. Appendix C: Details of Anticorrelation Function Calculation for the Case of Weak Measuement Performed on the 2-SELs

We refer to the Hamiltonian of 2-SEL system coupled to flying qubit given by equation (44) and we recognize that the time-dependent Hamiltonian $\hat{H}_{AC}(t)$ and evolution operator based on it is as follows

$$e^{\frac{1}{\hbar i}\int_0^t(\hat{H}_{AC}(t')\times\hat{I}_B)dt'} = \tag{56}$$

$$\begin{pmatrix} e^{\frac{1}{\hbar i}\int_0^t E_{c1''_1}(t')dt'} & 0 & 0 & 0 & 0 & 0 & 0 & 0 \\ 0 & e^{\frac{1}{\hbar i}\int_0^t E_{c1''_1}dt'} & 0 & 0 & 0 & 0 & 0 & 0 \\ 0 & 0 & e^{\frac{1}{\hbar i}\int_0^t E_{c2''_1}(t')dt'} & 0 & 0 & 0 & 0 & 0 \\ 0 & 0 & 0 & e^{\frac{1}{\hbar i}\int_0^t E_{c2''_1}(t')dt'} & 0 & 0 & 0 & 0 \\ 0 & 0 & 0 & 0 & e^{\frac{1}{\hbar i}\int_0^t E_{c1''_2}(t')dt'} & 0 & 0 & 0 \\ 0 & 0 & 0 & 0 & 0 & e^{\frac{1}{\hbar i}\int_0^t E_{c1''_2}(t')dt'} & 0 & 0 \\ 0 & 0 & 0 & 0 & 0 & 0 & e^{\frac{1}{\hbar i}\int_0^t E_{c2''_2}(t')dt'} & 0 \\ 0 & 0 & 0 & 0 & 0 & 0 & 0 & e^{\frac{1}{\hbar i}\int_0^t E_{c2''_2}dt'} \end{pmatrix}$$

Now we are defining the correlation function for 2-SELs in case of the system interaction with the external flying qubit given by the matrix

$$C_{AB,C} = \hat{I}_C \times \hat{C}_{AB} = \begin{pmatrix} 1 & 0 \\ 0 & 1 \end{pmatrix} \times \begin{pmatrix} 1 & 0 & 0 & 0 \\ 0 & -1 & 0 & 0 \\ 0 & 0 & -1 & 0 \\ 0 & 0 & 0 & 1 \end{pmatrix} = \begin{pmatrix} +1 & 0 & 0 & 0 & 0 & 0 & 0 & 0 \\ 0 & -1 & 0 & 0 & 0 & 0 & 0 & 0 \\ 0 & 0 & -1 & 0 & 0 & 0 & 0 & 0 \\ 0 & 0 & 0 & +1 & 0 & 0 & 0 & 0 \\ 0 & 0 & 0 & 0 & +1 & 0 & 0 & 0 \\ 0 & 0 & 0 & 0 & 0 & -1 & 0 & 0 \\ 0 & 0 & 0 & 0 & 0 & 0 & -1 & 0 \\ 0 & 0 & 0 & 0 & 0 & 0 & 0 & +1 \end{pmatrix}. \tag{57}$$

Now we construct Hamiltonian for non-interacting C and AB physical systems given as

$$\hat{H} = \hat{I}_C \times \hat{H}_{AB} + \hat{H}_C \times \hat{I}_{AB} =$$

$$= \begin{pmatrix} \hat{H}_{AB} & \hat{0}_{4\times4} \\ \hat{0}_{4\times4} & \hat{H}_{AB} \end{pmatrix} + \begin{pmatrix} \hat{H}_C[1,1] & 0 & 0 & 0 & \hat{H}_C[1,2] & 0 & 0 & 0 \\ 0 & \hat{H}_C[1,1] & 0 & 0 & 0 & \hat{H}_C[1,2] & 0 & 0 \\ 0 & 0 & \hat{H}_C[1,1] & 0 & 0 & 0 & \hat{H}_C[1,2] & 0 \\ 0 & 0 & 0 & \hat{H}_C[1,1] & 0 & 0 & 0 & \hat{H}_C[1,2] \\ \hat{H}_C[2,1] & 0 & 0 & 0 & \hat{H}_C[2,2] & 0 & 0 & 0 \\ 0 & \hat{H}_C[2,1] & 0 & 0 & 0 & \hat{H}_C[2,2] & 0 & 0 \\ 0 & 0 & \hat{H}_C[2,1] & 0 & 0 & 0 & \hat{H}_C[2,2] & 0 \\ 0 & 0 & 0 & \hat{H}_C[2,1] & 0 & 0 & 0 & \hat{H}_C[2,2] \end{pmatrix} =$$

$$= \begin{pmatrix} E_{p1}+E_{p1'}+E_{c1} & t_{s1'2'} & t_{s12} & 0 & 0 & 0 & 0 & 0 \\ t^*_{s1'2'} & E_{p1}+E_{p2'}+E_{c2} & 0 & t_{s12} & 0 & 0 & 0 & 0 \\ t^*_{s12} & 0 & E_{p2}+E_{p1'}+E_{c2} & t_{s1'2'} & 0 & 0 & 0 & 0 \\ 0 & t^*_{s12} & t^*_{s1'2'} & E_{p2}+E_{p2'}+E_{c1} & 0 & 0 & 0 & 0 \\ 0 & 0 & 0 & 0 & E_{p1}+E_{p1'}+E_{c1} & t_{s1'2'} & t_{s12} & 0 \\ 0 & 0 & 0 & 0 & t^*_{s1'2'} & E_{p1}+E_{p2'}+E_{c2} & 0 & t_{s12} \\ 0 & 0 & 0 & 0 & t^*_{s12} & 0 & E_{p2}+E_{p1'}+E_{c2} & t_{s1'2'} \\ 0 & 0 & 0 & 0 & 0 & t_{s12} & t^*_{s1'2'} & E_{p2}+E_{p2'}+E_{c1} \end{pmatrix} +$$

$$+ \begin{pmatrix} E_{p1''} & 0 & 0 & 0 & t_{s1''2''} & 0 & 0 & 0 \\ 0 & E_{p1''} & 0 & 0 & 0 & t_{s1''2''} & 0 & 0 \\ 0 & 0 & E_{p1''} & 0 & 0 & 0 & t_{s1''2''} & 0 \\ 0 & 0 & 0 & E_{p1''} & 0 & 0 & 0 & t_{s1''2''} \\ t^*_{s1''2''} & 0 & 0 & 0 & E_{p2''} & 0 & 0 & 0 \\ 0 & t^*_{s1''2''} & 0 & 0 & 0 & E_{p2''} & 0 & 0 \\ 0 & 0 & t^*_{s1''2''} & 0 & 0 & 0 & E_{p2''} & 0 \\ 0 & 0 & 0 & t^*_{s1''2''} & 0 & 0 & 0 & E_{p2''} \end{pmatrix} =$$

$$\begin{pmatrix} E_{p1}+E_{p1'}+E_{c1} & t_{s1'2'} & t_{s12} & 0 & t_{s1''2''} & 0 & 0 & 0 \\ t^*_{s1'2'} & E_{p1}+E_{p2'}+E_{c2} & 0 & t_{s12} & 0 & t_{s1''2''} & 0 & 0 \\ t^*_{s12} & 0 & E_{p2}+E_{p1'}+E_{c2} & t_{s1'2'} & 0 & 0 & t_{s1''2''} & 0 \\ 0 & t^*_{s12} & t^*_{s1'2'} & E_{p2}+E_{p2'}+E_{c1} & 0 & 0 & 0 & t_{s1''2''} \\ t^*_{s1''2''} & 0 & 0 & 0 & E_{p1}+E_{p1'}+E_{c1} & t_{s1'2'} & t_{s12} & 0 \\ 0 & t^*_{s1''2''} & 0 & 0 & t^*_{s1'2'} & E_{p1}+E_{p2'}+E_{c2} & 0 & t_{s12} \\ 0 & 0 & t^*_{s1''2''} & 0 & t^*_{s12} & 0 & E_{p2}+E_{p1'}+E_{c2} & t_{s1'2'} \\ 0 & 0 & 0 & t^*_{s1''2''} & 0 & t_{s12} & t^*_{s1'2'} & E_{p2}+E_{p2'}+E_{c1} \end{pmatrix} +$$

$$+ diag(E_{p1''}, E_{p1''}, E_{p1''}, E_{p1''}, E_{p2''}, E_{p2''}, E_{p2''}, E_{p2''}).$$

We recognize that diagonal elements of $\hat{I}_C \times \hat{H}_{AB} + \hat{H}_C \times \hat{I}_{AB}$ are

$$(E_{p1}+E_{p1'}+E_{c1}+E_{p1''}, E_{p1}+E_{p2'}+E_{c2}+E_{p1''}, E_{p2}+E_{p1'}+E_{c2}+E_{p1''}, E_{p2}+E_{p2'}+E_{c1}+E_{p1''},$$
$$E_{p1}+E_{p1'}+E_{c1}+E_{p2''}, E_{p1}+E_{p2'}+E_{c2}+E_{p2''}, E_{p2}+E_{p1'}+E_{c2}+E_{p2''}, E_{p2}+E_{p2'}+E_{c1}+E_{p2''}).$$

Now we consider the interaction between qubits C and A denoted by H_{CA} and it will be incoroporated into global Hamiltonian $\hat{H}_{CA} \times \hat{I}_B$ that has the following diagonal matrix representation

$$\hat{H}_{CA} = \begin{pmatrix} E_{c1''1}(t) & 0 & 0 & 0 \\ 0 & E_{c1''2}(t) & 0 & 0 \\ 0 & 0 & E_{c2''1}(t) & 0 \\ 0 & 0 & 0 & E_{c2''2}(t) \end{pmatrix} \tag{58}$$

and consequently

$$\hat{H}_{CA} \times \hat{I}_B = \begin{pmatrix} E_{c1''1}(t) & 0 & 0 & 0 & 0 & 0 & 0 & 0 \\ 0 & E_{c1''1}(t) & 0 & 0 & 0 & 0 & 0 & 0 \\ 0 & 0 & E_{c1''2}(t) & 0 & 0 & 0 & 0 & 0 \\ 0 & 0 & 0 & E_{c1''2}(t) & 0 & 0 & 0 & 0 \\ 0 & 0 & 0 & 0 & E_{c2''1}(t) & 0 & 0 & 0 \\ 0 & 0 & 0 & 0 & 0 & E_{c2''1}(t) & 0 & 0 \\ 0 & 0 & 0 & 0 & 0 & 0 & E_{c2''2}(t) & 0 \\ 0 & 0 & 0 & 0 & 0 & 0 & 0 & E_{c2''2}(t) \end{pmatrix}. \tag{59}$$

We have the total Hamiltonian for the flying qubit interacting with 2-SELs given as

$$\hat{H} = \hat{I}_C \times \hat{H}_{AB} + \hat{H}_C \times \hat{I}_{AB} + \hat{H}(t)_{CA} \times \hat{I}_B. \tag{60}$$

We recognize that the diagonal terms of total matrix are given as a following sequence
$(E_{p1}+E_{p1'}+E_{c1}+E_{p1''}+E_{c1''1}(t), E_{p1}+E_{p2'}+E_{c2}+E_{p1''}+E_{c1''1}(t), E_{p2}+E_{p1'}+E_{c2}+E_{p1''}+E_{c1''2}(t), E_{p2}+E_{p2'}+E_{c1}+E_{p1''}+E_{c1''2}(t),$
$E_{p1}+E_{p1'}+E_{c1}+E_{p2''}+E_{c2''1}(t), E_{p1}+E_{p2'}+E_{c2}+E_{p2''}+E_{c2''1}(t), E_{p2}+E_{p1'}+E_{c2}+E_{p2''}+E_{c2''2}(t), E_{p2}+E_{p2'}+E_{c1}+E_{p2''}+E_{c2''2}(t))$. Setting $E_{p1} = E_{p1'} = E_{p1''} = E_{p2} = E_{p2'} = E_{p2''} = E_p$, we obtain diagonal terms as

$$(E_{c1}+3E_p+E_{c1''1}(t), E_{c2}+3E_p+E_{c1''1}(t), E_{c2}+3E_p+E_{c1''2}(t), 3E_p+E_{c1}+E_{c1''2}(t),$$
$$E_{c1}+3E_p+E_{c2''1}(t), 3E_p+E_{c2}+E_{c2''1}(t), 3E_p+E_{c2}+E_{c2''2}(t), 3E_p+E_{c1}+E_{c2''2}(t)). \tag{61}$$

Substracting element $3E_p + E_{c1}$ we obtain

$$E_{c1''1}(t), E_{c2}-E_{c1}+E_{c1''1}(t), E_{c2}-E_{c1}+E_{c1''2}(t), E_{c1''2}(t),$$
$$E_{c2''1}(t), E_{c2}-E_{c1}+E_{c2''1}(t), E_{c2}-E_{c1}+E_{c2''2}(t), E_{c2''2}(t)). \tag{62}$$

Now we are constructing the density matrix for the case of non-interacting qubit C with 2-SELs denoted as AB system. We assume that qubit C is in the ground state and that symmetric 2-SELs line is populated at energy E_1 or E_2. In such a case, the density matrices are as follows

$$\hat{\rho}_C = \begin{pmatrix} +\frac{1}{2} & -\frac{1}{2} \\ -\frac{1}{2} & +\frac{1}{2} \end{pmatrix}, \hat{\rho}_{AB} = \begin{pmatrix} +\frac{1}{2} & 0 & 0 & -\frac{1}{2} \\ 0 & 0 & 0 & 0 \\ 0 & 0 & 0 & 0 \\ -\frac{1}{2} & 0 & 0 & +\frac{1}{2} \end{pmatrix} \tag{63}$$

Therefore, the density matrix of non-interacting qubit C with 2-SELs line denoted as AB system is given as

$$\hat{\rho}_{ABC} = \begin{pmatrix} +\frac{1}{2} & -\frac{1}{2} \\ -\frac{1}{2} & +\frac{1}{2} \end{pmatrix} \times \begin{pmatrix} +\frac{1}{2} & 0 & 0 & -\frac{1}{2} \\ 0 & 0 & 0 & 0 \\ 0 & 0 & 0 & 0 \\ -\frac{1}{2} & 0 & 0 & +\frac{1}{2} \end{pmatrix} = \begin{pmatrix} +\frac{1}{4} & 0 & 0 & -\frac{1}{4} & -\frac{1}{4} & 0 & 0 & +\frac{1}{4} \\ 0 & 0 & 0 & 0 & 0 & 0 & 0 & 0 \\ 0 & 0 & 0 & 0 & 0 & 0 & 0 & 0 \\ -\frac{1}{4} & 0 & 0 & +\frac{1}{4} & +\frac{1}{4} & 0 & 0 & -\frac{1}{4} \\ -\frac{1}{4} & 0 & 0 & +\frac{1}{4} & +\frac{1}{4} & 0 & 0 & -\frac{1}{4} \\ 0 & 0 & 0 & 0 & 0 & 0 & 0 & 0 \\ 0 & 0 & 0 & 0 & 0 & 0 & 0 & 0 \\ +\frac{1}{4} & 0 & 0 & -\frac{1}{4} & -\frac{1}{4} & 0 & 0 & +\frac{1}{4} \end{pmatrix}. \tag{64}$$

The density matrix follows the equation of motion

$$\rho(t) = e^{\frac{1}{i\hbar}\int_0^t H(t')dt'} \begin{pmatrix} +\frac{1}{4} & 0 & 0 & -\frac{1}{4} & -\frac{1}{4} & 0 & 0 & +\frac{1}{4} \\ 0 & 0 & 0 & 0 & 0 & 0 & 0 & 0 \\ 0 & 0 & 0 & 0 & 0 & 0 & 0 & 0 \\ -\frac{1}{4} & 0 & 0 & +\frac{1}{4} & +\frac{1}{4} & 0 & 0 & -\frac{1}{4} \\ -\frac{1}{4} & 0 & 0 & +\frac{1}{4} & +\frac{1}{4} & 0 & 0 & -\frac{1}{4} \\ 0 & 0 & 0 & 0 & 0 & 0 & 0 & 0 \\ 0 & 0 & 0 & 0 & 0 & 0 & 0 & 0 \\ +\frac{1}{4} & 0 & 0 & -\frac{1}{4} & -\frac{1}{4} & 0 & 0 & +\frac{1}{4} \end{pmatrix} e^{-\frac{1}{i\hbar}\int_0^t H(t')dt'}. \tag{65}$$

Since the structure of the Hamiltonian matrix $\hat{H}(t) = \hat{I}_C \times \hat{H}_{AB} + \hat{H}_C \times \hat{I}_{AB} + \hat{H}_{CA}(t) \times \hat{I}_B$ describing the interaction of three electrons confined to the flying position-based qubit C and 2-SEL system is known at all instances of time in the analytical way as well as the operators $e^{\pm\frac{1}{i\hbar}\int_0^t H(t')dt'}$ are known in the analytical way, the structure of the density matrix is known in the analytical way. This implies our full knowledge of the qubit C state and 2-SELs system at any instance of time thanks to the formula (41). Such reasoning opens the perspective of analytical approach towards quantum N-body electron (hole) system confined to the three disconnected graphs of quantum dots of any topology in the 3D space subjected to the steering mechanism from voltage polarization applied to CMOS gates, as depicted in Fig.1. It is thus the subject of the future more detailed studies with use of both analytical and numerical tools. It also opens the perspective on new experiments and new technological novelties in the area of cryogenic CMOS single-electron device electronics that have both importance in the implementation of quantum computer as well as in the development of classical single electron electronics.

REFERENCES

[1] B.Patra, R.Incandela, J.Van Dijk, H.Homulle, L.Song, M.Shahmohammadi, R.B.Staszewski, and et al., "Cryo-cmos circuits and systems for quantum computing applications," IEEE Journal of Solid-State Circuits, 53(1):309–321, 2018.

[2] P. Giounanlis, E. Blokhina, K. Pomorski, D. R. Leipold, and R. B. Staszewski, "Modeling of semiconductor electrostatic qubits realized through coupled quantum dots," IEEE Access, pages 1–16, 2019.

[3] K.Pomorski, P.Giounanlis, E.Blokhina, P.Peczkowski, D.Leipold, B.Staszewski, Superconductivity and Particle Accelerators 2018, Proc. SPIE 11054, 110540M, 2019); doi: 10.1117/12.2525217

[4] K.Pomorski, H.Akaike, A.Fujimaki, and K.Rusek, "Relaxation method in description of ram memory cell in rsfq computer," COMPEL, 38(1):395–414, 2019

[5] D. Leipold, H. Leipold, L. Leipold, E. Blokhina, P. Giounanlis, K. Pomorski, R. Staszewski, I. Bashir, G. Maxim, M. Asker, C. Cetintepe, A. Esmailiyan, H. Wang, and T. Siriburanon, "Implementation and Simulation of Electrostatically Controlled Quantum Dots in CMOS Technology," *American Physical Society (APS) Meeting*, 6 Mar. 2019, ses. P35.12, pp. 1–1, Boston, Massachusetts, USA. [Meeting link]

[6] M.-S. Choi, J. Yi, M. Y. Choi, J. Choi, and S.-I. Lee, "Quantum phase transitions in josephson-junction chains," Phys. Rev. B, 57:R716–R719, 1998.

[7] H. Q. Xu, "Method of calculations for electron transport in multiterminal quantum systems based on real-space lattice models," Phys. Rev. B, 66:165305,

[8] T. Fujisawa, T. Hayashi, HD Cheong, YH Jeong, and Y. Hirayama, "Rotation and phase-shift operations for a charge qubit in a double quantum dot," Physica E: Low-dimensional Systems and Nanostructures, 21(2-4):1046–1052, 2004.

[9] K. D. Petersson, J. R. Petta, H. Lu, and A. C. Gossard, "Quantum coherence in a one-electron semiconductor charge qubit," Phys. Rev. Lett., 105:246804, 2010.
[10] P. Giounanlis, E. Blokhina, D. Leipold and R. B. Staszewski, "Occupancy Oscillations and Electron Transfer in Multiple-Quantum-Dot Qubits and their Circuit Representation," 2018 25th IEEE International Conference on Electronics, Circuits and Systems (ICECS), Bordeaux, 2018, pp. 153-156, doi: 10.1109/ICECS.2018.8618063
[11] Jozef Spalek, "Wstep do fizyki materii skondensowanej," PWN, 2015
[12] D. Maile, S. Andergassen, and W. Belzig, "Quantum phase transition with dissipative frustration," Phys. Rev. B, 97, 2018.
[13] S. Sachdev, "Quantum phase transitions", Cambridge Univ. Press, 2011.
[14] Wolfram Mathematica: $http://www.wolfram.com/mathematica/$
[15] Wikipedia:Bell theorem